CHAPTER TWO

PIFAs for Internal Mobile Phone Antennas

2.1 INTRODUCTION

In comparison to the conventional protruded whip or rod antennas for applications in mobile phones, there are two major advantages of PIFAs: One advantage is that PIFAs are concealable within the housing of the mobile phones, and the other is that they capable of having reduced backward radiation toward the user's head to reduce electromagnetic wave power absorption and enhance antenna performance. Owing to these advantages, many PIFA designs have been devised, especially for achieving dual-frequency operations for applications in GSM/DCS dual-band or GSM/DCS/PCS triple-band mobile phones [1–14]. Design examples of the dual-frequency PIFAs using various promising techniques are described in Section 2.2, and detailed design considerations and experimental results are presented.

PIFA designs capable of triple-frequency operations in the 900, 1800, and 2450 MHz bands for GSM, DCS, and WLAN applications are also available in the open literature [15–17], in which the techniques of using two or three separate patches, a meandered patch, and a branch-line strip with a folded end have been applied. The related designs are addressed in Section 2.3. In Section 2.4, an interesting design of using an L-shaped ground plane to replace the conventional flat ground plane for PIFAs is described [18]. Such PIFAs can have further reduced backward radiation and enhanced antenna gain.

The techniques of using stacked PIFAs to achieve wider impedance bandwidths [19, 20] are discussed in Section 2.5. Finally, significant effects of ground plane dimensions on the impedance bandwidth of the PIFA are demonstrated. Experimental results of a constructed prototype for a UMTS mobile phone showed that

the PIFA can have an impedance bandwidth varying from about 150 to 490 MHz, a variation of more than 300% [21]. The detailed results are presented and discussed in Section 2.6.

2.2 DUAL-FREQUENCY PIFA

2.2.1 Two Separate Patches with a Dual-Feed Design

Figure 2.1 shows the top patch of the PIFA comprising two separate patches of different sizes for achieving 900 and 1800 MHz operations. Note that the larger and smaller patches have separate shorting points and are operated, respectively, in the 900 and 1800 MHz bands as quarter-wavelength resonant structures. A dual feed (feed point 1 for the larger patch and feed point 2 for the smaller patch) is also utilized in the design, which can find application where mobile phones have receivers with dual front ends. In addition, to achieve a compact antenna size, a portion of the larger patch is removed to accommodate the smaller patch. Related studies have been reported in References 1 and 2]. A compact 900/1800 MHz dual-frequency PIFA with an area of $25 \times 26\,\text{mm}^2$ and a height of 4 mm has been studied in Reference 2, in which the PIFA has a capacitive load and is fed by a capacitive feed and in addition, a dielectric substrate with a relative permittivity of 2.1 is used between the two top patches and the ground plane.

2.2.2 Patch with an L-Shaped or Folded Slit

Figure 2.2 shows two promising designs of the top patch of the dual-frequency PIFA using a single probe feed and a common shorting pin. In Figure 2.2a, with the use of an L-shaped slit inserted at the patch boundary [3], the rectangular top patch can be separated into two subpatches of different sizes. The dimensions of the larger and the smaller subpatches can be designed to roughly resonate as a quarter-wavelength structure to operate in the 900 and 1800 MHz bands, respectively. Two subpatches can also be obtained by using a folded slit [4, 5], as shown in Figure 2.2b. Note that, in this case, the resonant path provided by the smaller subpatch starts from the feed point and then extends into the center portion of the rectangular patch. A large portion of this resonant path is thus surrounded by the outer larger subpatch,

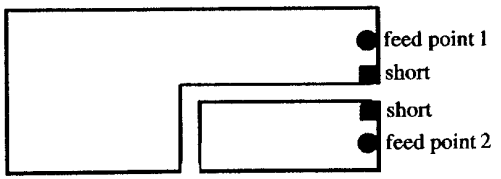

FIGURE 2.1 Top patch of the dual-frequency PIFA comprising two separate patches for achieving 900 and 1800 MHz operations.

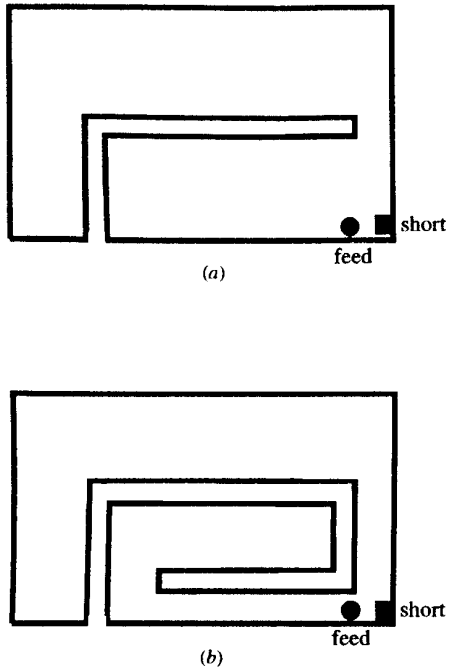

FIGURE 2.2 Top patch of the dual-frequency PIFA with (a) an L-shaped slit and (b) a folded slit.

which has the advantage of obtaining reduced backward radiation, leading to a smaller electromagnetic wave power absorption by the user's head in the 1800 MHz band operation.

2.2.3 Patch with a U-Shaped Slot

Recently, instead of using an L-shaped slit or a folded slit to obtain two separate subpatches in the radiating top patch, a design using an embedded U-shaped slot (see Fig. 2.3) has been used [6, 7]. In this design, a smaller rectangular patch of dimensions $L_2 \times W_2$ for operating in the 1800 MHz band is obtained in the central portion of the original rectangular patch of dimensions $L_1 \times W_1$, which is for the 900 MHz band operation. Because the smaller rectangular patch is embedded within the radiating top patch, it is also expected that this design can provide reduced electromagnetic wave power absorption by the user's head in the 1800 MHz band. The lower (f_1) and upper (f_2) operating frequencies of this PIFA design can also be approximately determined from

$$f_1 \cong \frac{c}{4(L_1 + W_1)}, \tag{2.1}$$

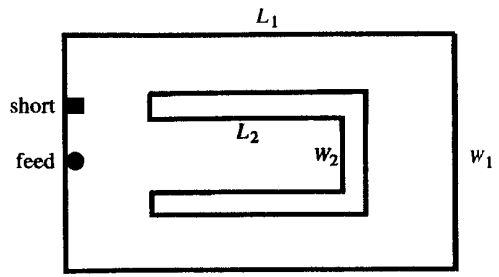

FIGURE 2.3 Top patch of the dual-frequency PIFA with an embedded U-shaped slot.

$$f_2 \cong \frac{c}{4(L_2 + W_2)}. \tag{2.2}$$

The above two equations make the design of such a dual-frequency PIFA easy to achieve, and c in the equations is the speed of light in free space.

2.2.4 Patch with a Branch Line Slit

The designs shown in Sections 2.2.1–2.2.3 mainly utilize two different resonant paths for dual-frequency operation (the smaller one for the 1800 MHz band and the larger one for the 900 MHz band). Figure 2.4 shows another promising PIFA design to achieve 900/1800 MHz dual-frequency operations. This design utilizes

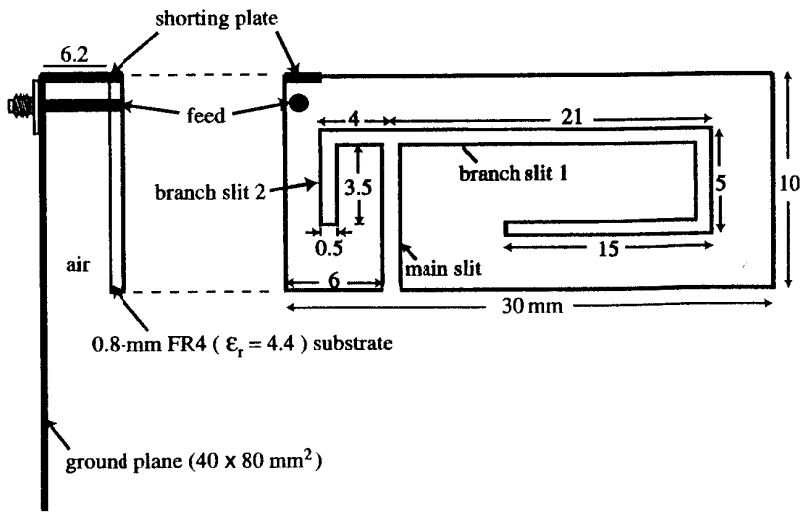

FIGURE 2.4 Geometry of the dual-frequency PIFA with a branch-line slit; dimensions given in the figure are in millimeters. (From Ref. 8, © 2002 John Wiley & Sons, Inc.)

an asymmetric branch-line slit to meander the excited patch surface currents in the top patch, which leads to a large reduction in the required top patch dimensions of the PIFA, and the first two resonant frequencies of the meandered resonant path are also tuned to obtain 900 and 1800 MHz operations.

A prototype based on the design dimensions shown in Figure 2.4 has been constructed and tested [8]. The top patch is printed on a 0.8-mm FR4 substrate and short-circuited to the antenna's ground plane with a shorting plate of length 2 mm. A branch-line slit consisting of a main slit, a long folded branch slit (branch slit 1 in the figure), and a short bent branch slit (branch slit 2 in the figure) is embedded in the top patch. The main slit, which has an open end at the patch boundary, and the long folded branch slit in the top patch are mainly for effectively meandering the excited patch surface currents. On the other hand, the short bent branch slit is mainly for achieving enhanced impedance matching of the first two excited resonant frequencies to obtain wider operating bandwidths. Also note that the required length of the short bent branch slit is much smaller than that of the long folded branch slit. The feed point is located close to the shorting plate, and both the feed point and the shorting plate are also required to be placed at the patch edge near the short bent branch slit. In this case, a large meandering of the excited patch surface currents starting from the feed point to the portion of the patch encircled by the long folded branch slit can be obtained. This large meandering leads to a large reduction in the required patch dimensions for the proposed 900/1800 MHz band operations.

It should also be noted that the wavelengths of the first two resonant frequencies in this PIFA design correspond, respectively, to about 4.0 and 2.0 times the length of the meandered patch surface current path, starting from the feed point to the portion of the patch encircled by the long folded branch slit. That is, this meandered patch portion is operated as a radiator with resonant lengths of about 0.25 and 0.5 wavelengths in the proposed design. This characteristic also makes it very convenient in achieving the 900 and 1800 MHz excitation for this PIFA design. In addition, because the end portion of the meandered patch surface current path, encircled by the folded branch slit, is in the central portion of the top patch, lower electromagnetic wave power absorption by the user's head in both the 900 and 1800 MHz bands can be expected. A specific absorption rate (SAR) measurement on a design very similar to that shown in Figure 2.4 showed a very low SAR level of 0.21 W/kg at 900 MHz and an even lower SAR level of 0.11 W/kg at 1800 MHz. The measured results confirm this expectation.

Figure 2.5 shows the measured and simulated return loss for the constructed prototype based on the design dimensions shown in Figure 2.4. The simulation results, which agree well with the measured data, are obtained by using IE3D simulation software. From the results obtained, the first two resonant frequencies at about 900 and 1800 MHz are excited with good impedance matching. The measured bandwidths, determined from 2.5:1 VSWR or about 7.3 dB return loss, are about 24 and 123 MHz in the 900 and 1800 MHz bands, respectively, which are comparable to those obtained in Reference 9, although the constructed prototype has a much smaller antenna volume of only $30\times10\times7\ \text{mm}^3$. However, it should be

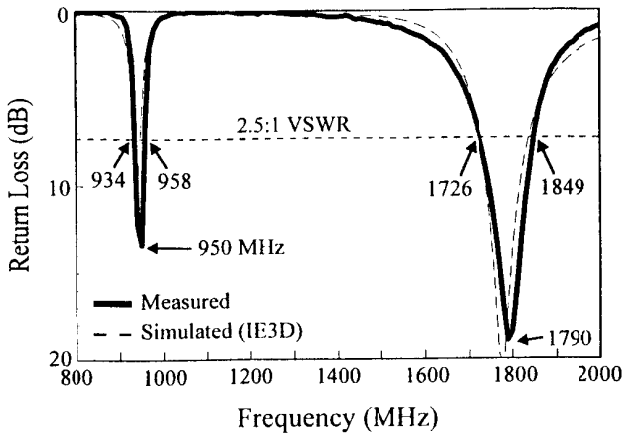

FIGURE 2.5 Measured and simulated return loss of the PIFA shown in Figure 2.4. (From Ref. 8, © 2002 John Wiley & Sons, Inc.)

noted that the obtained bandwidths are still not large enough to meet the bandwidth requirements of the GSM/DCS cellular communications systems [70 MHz (890–960 MHz) and 170 MHz (1710–1880 MHz) for the GSM and DCS systems, respectively]. Further enhancement in the impedance bandwidths is required to obtain optimal performance for GSM/DCS mobile phones.

The excited patch surface current distributions in the top patch for the two resonant frequencies have also been studied. Figure 2.6 shows the simulation results of the excited patch surface currents at resonance of the two excited resonant modes. It is seen that the current path, which starts from the feed point to the portion of the patch encircled by the long folded branch slit, determines the excitation of the two desired resonant frequencies. The patch portion with this current path thus acts as a main radiator in this PIFA design to resonate at 0.25 and 0.5 wavelengths. In this design, the length (ℓ) of this meandered current path is about 80 mm. That is, the first or lower frequency for the proposed antenna has a wavelength corresponding to be about 4.0ℓ, and the second or upper frequency has a wavelength of about 2.0ℓ.

Figures 2.7 and 2.8 plot the measured radiation patterns at two resonances of the antenna. For both resonant frequencies, good omnidirectional radiation in the azimuthal plane (x–z plane) is seen. The antenna gain is also measured to be about 0.5 and 1.5 dBi for the lower and upper resonant frequencies, respectively.

2.2.5 Meandered Patch With/Without a Parasitic Shorted Patch

By properly meandering the top patch of the PIFA, the frequency ratio of the PIFA's first two resonant frequencies can be tuned to be about 2.0, which makes it very promising for obtaining the 900 and 1800 MHz operations [9, 10]. By further incor-

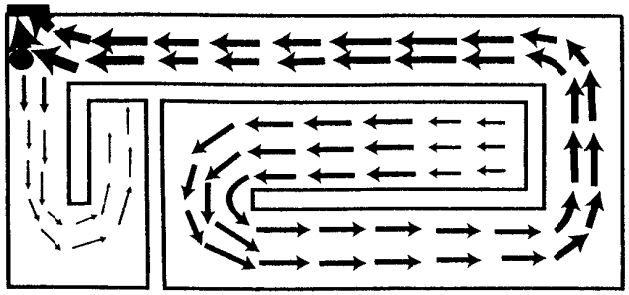

(a) $f = 950$ Mhz

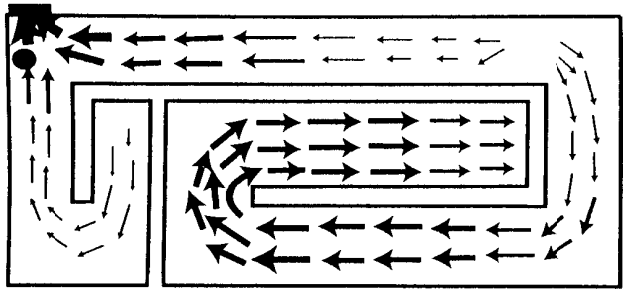

(b) $f = 1790$ Mhz

FIGURE 2.6 Simulated patch surface current distributions (IE3D simulation results) at (a) $f = 950$ MHz and (b) $f = 1790$ MHz for the PIFA shown in Figure 2.4. (From Ref. 8, © 2002 John Wiley & Sons, Inc.)

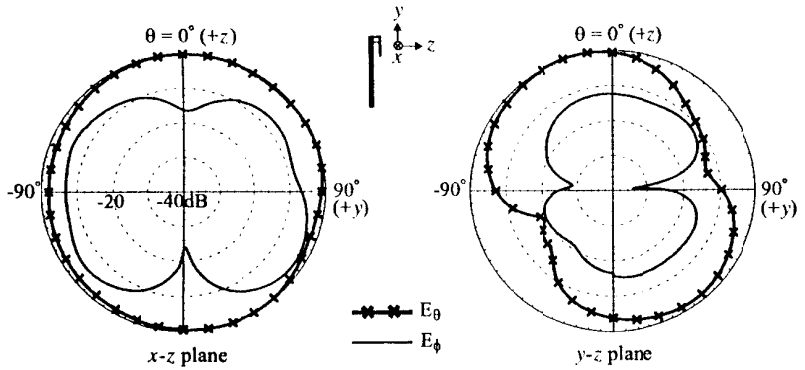

FIGURE 2.7 Measured radiation patterns at 950 MHz for the PIFA shown in Figure 2.4. (From Ref. 8, © 2002 John Wiley & Sons, Inc.)

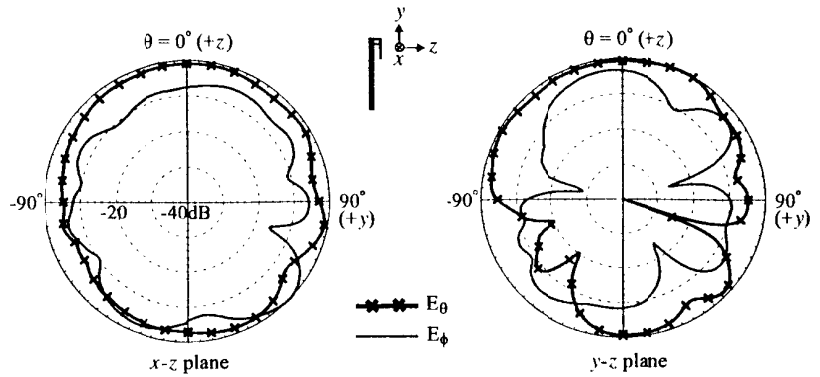

FIGURE 2.8 Measured radiation patterns at 1790 MHz for the PIFA shown in Figure 2.4. (From Ref. 8, © 2002 John Wiley & Sons, Inc.)

porating the use of a parasitic shorted patch (see the geometry shown in Fig. 2.9), a much enhanced bandwidth in the upper band of the PIFA has also been demonstrated [10]. In this design, with the PIFA occupying a volume of $40 \times 30.4 \times 7.2\,\text{mm}^3$ and mounted on the top portion of a ground plane having an area of $40 \times 110\,\text{mm}^2$, the obtained impedance bandwidth, determined by 6 dB return loss (3:1 VSWR), reaches 535 MHz in the upper band, covering the required bandwidth of the DCS and PCS operations. This relatively larger upper band bandwidth is mainly due to the added parasitic shorted patch, which introduces an additional resonant mode to the upper band and makes the upper band become a dual-resonance band. This condition leads to an enhanced impedance bandwidth. In addition, this design has a sufficient bandwidth in the lower band (about

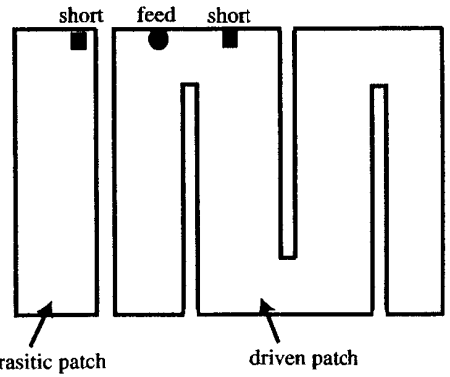

FIGURE 2.9 Top patch of the dual-frequency PIFA with a meandered patch and a parasitic shorted patch.

115 MHz) to cover the required bandwidth of the GSM operation. In this case, the obtained PIFA design is suitable for applications in GSM/DCS/PCS triple-band mobile phones. A similar design using a parasitic shorted patch to obtaining a PIFA capable of GSM/DCS/PCS triple-band operations has also been shown in Reference 11.

2.2.6 Two or More Shorted Patches or Strips

By using two or more shorted patches with a common shorting pin, bandwidth enhancement in both the lower and upper bands of the PIFA has been obtained. A promising design is shown in Figure 2.10. This design utilizes a folded slit-loaded patch (patch 1) and a folded patch (patch 2), both sharing a common shorting pin. The two patches are printed on the same FR4 supporting substrate of thickness 0.8 mm and relative permittivity 4.4. Patch 2 is also configured to be around patch 1 to result in a compact size for the PIFA. In this design, the two patches occupy a small area of $18 \times 32\ \text{mm}^2$ and an air layer of thickness 6.4 mm is between the ground plane and the supporting FR4 substrate; that is, the total antenna height is 7.2 mm. The two patches are excited by a probe feed located close to the common shorting pin.

Notice that a folded slit, as discussed in Section 2.2.2, is embedded in patch 1. This folded slit separates patch 1 into two subpatches of different sizes, which generate a resonant mode in each of the 900 and 1800 MHz bands. On the other

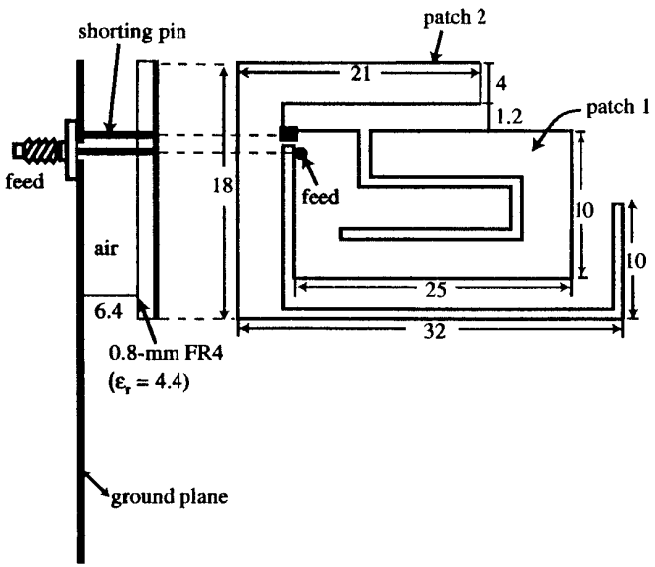

FIGURE 2.10 Geometry of the dual-frequency PIFA with a folded-slit-loaded patch and a folded patch.

hand, because of the shorting pin loading, it is possible for patch 2 to operate as either a quarter-wavelength or a half-wavelength antenna [22, 23]. This behavior has been confirmed in experiments, and through adjustments of the dimensions of patch 2 this PIFA design can have two additional resonant modes excited, one close to the 900 MHz band and one close to the 1800 MHz band. Thus, by incorporating the two resonant modes excited by patch 1, the proposed PIFA can have two resonant modes excited in each of its lower and upper bands. This behavior not only gives the proposed PIFA sufficient operating bandwidths for the GSM and DCS systems but also makes it possible to cover the additional frequency band of the PCS system, leading to a GSM/DCS/PCS triple-band PIFA.

Figure 2.11 shows the geometry of a related promising PIFA design. In this case, three resonant elements are used: two meandered metallic strips of slightly different lengths (strips 1 and 2) and one nearly rectangular patch (patch 1), which are printed

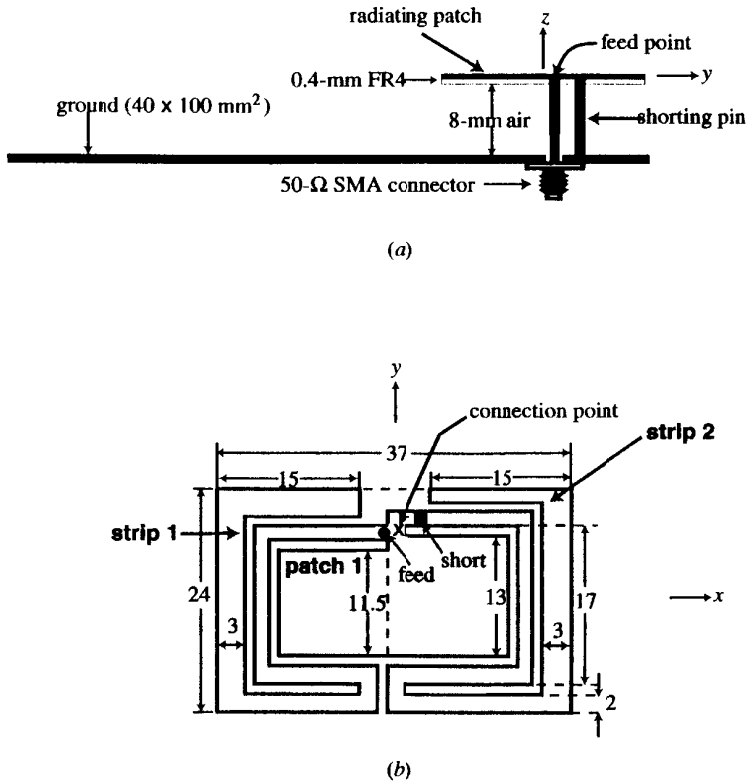

FIGURE 2.11 Geometry of the dual-frequency PIFA with two shorted strips and one shorted patch. (a) Side view of the PIFA mounted on the top portion of a ground plane of dimensions $40 \times 100\ \text{mm}^2$; (b) top patch of the PIFA. (From Ref. 12, © 2002 IEEE, reprinted with permission)

on a same supporting FR4 substrate (thickness 0.4 mm and relative permittivity 4.4) and arranged in a compact configuration. These three resonant elements share a common shorting pin, and for the GSM operation in the lower band, the proposed PIFA is operated with the two meandered strips both resonated as quarter-wavelength structures, leading to a wide bandwidth formed by two resonant modes. For the DCS operation in the upper band, three resonant modes are generated, two from the second higher-order modes of the two meandered strips and one from the nearly rectangular patch, leading to a wide bandwidth covering the DCS band.

Also note that the three resonant elements are excited by a common probe feed at a position close to the connection point. Patch 1 is a nearly rectangular patch and is placed in the center. Note that the use of a nearly rectangular patch, instead of a simple rectangular patch, in this design is for fine-tuning the PIFA's lower and upper bands to exactly cover the GSM and DCS bands, respectively. The dimensions of patch 1 are selected such that it will generate a resonant mode at about 1900 MHz to widen the operating bandwidth of the upper band. The dimensions of patch 1 can also be roughly determined from Equation 2.1 or Equation 2.2.

Strips 1 and 2 have slightly different lengths (about 84 and 86 mm for strips 1 and 2, respectively, in this design) and are meandered around the left and right boundaries of patch 1, with a gap of 1 mm. In the proposed design, the first two resonant modes of strips 1 and 2 can be successfully excited. The first or the fundamental resonant mode of strips 1 and 2 is designed to occur at about 930 and 900 MHz, respectively. In this case, strips 1 and 2 are both operated as quarter-wavelength structures; that is, the lengths (ℓ) of strips 1 and 2 can be roughly determined from

$$f_0 = \frac{c}{4\ell}, \tag{2.3}$$

where c is again the speed of light in free space and f_0 is the desired resonant frequency.

At the same time, it is found that the second higher-order mode, whose resonant frequency is about 1.9 times that of the fundamental resonant frequency, of strips 1 and 2 can also be excited. The two excited second higher-order modes incorporating the resonant mode associated with patch 1 form a wide impedance bandwidth for the DCS operation. Also note that the widths of the two strips are not constants. The variations in the strip widths can affect the occurrence of the resonant modes of the PIFA, and their optimal dimensions can be obtained with the aid of the simulation software Ansoft HFSS (high-frequency structure simulator).

A prototype of the PIFA design shown in Figure 2.11 was constructed and studied. The PIFA is mounted on the top portion of a ground plane of width 40 mm and length 100 mm, which can be considered to be the ground plane of a practical mobile phone. Figure 2.12 shows the measured and simulated return loss for the constructed prototype. Reasonable agreement between the measured data and the simulated results is obtained. For the lower band, two resonant modes are

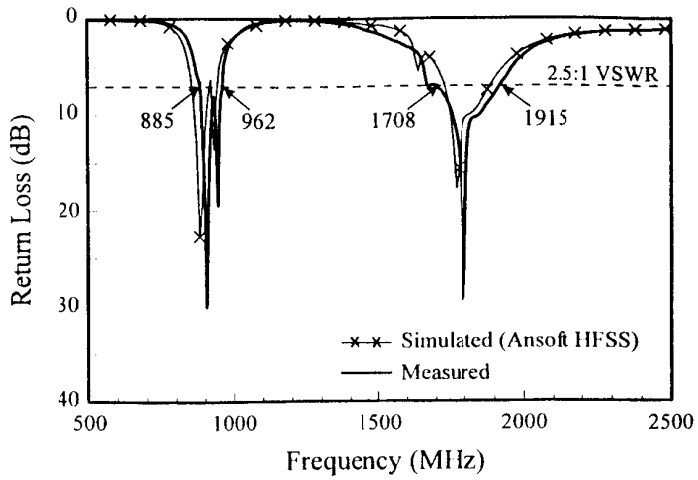

FIGURE 2.12 Measured and simulated return loss of the PIFA shown in Figure 2.11. (From Ref. 12, © 2002 IEEE, reprinted with permission)

successfully excited as expected, and an impedance bandwidth, determined from 2.5:1 VSWR or about 7.3 dB return loss, of 77 MHz (885–962 MHz) is obtained which meets the required bandwidth of the GSM system. For the upper band three resonant modes are seen to be excited, also as expected. Also note that the first two resonances at about 1.7 and 1.8 GHz in the upper band are greatly controlled by the lengths of strips 2 and 1, respectively. As for the third resonance at about 1.9 GHz, it is greatly affected by the dimensions of patch 1. The impedance bandwidth obtained is as large as 207 MHz (1708–1915 MHz), which covers the required bandwidth of the DCS system.

The radiation characteristics of the proposed PIFA have also been studied. Figure 2.13 plots the measured radiation patterns at the center frequencies of the GSM and DCS bands. The measured patterns show a better front-to-back ratio at 1795 MHz than at 925 MHz. The measured antenna gain for operating frequencies in the GSM and DCS bands is presented in Figure 2.14. For the GSM band, the peak antenna gain reaches about 2.7 dBi, with gain variations within 1.7 dBi. As for the DCS band, the peak antenna gain is about 2.1 dBi and the gain variations are less than 1.1 dBi.

2.2.7 Meandered Patch with a Folded End

To reduce the size of the dual-frequency PIFA, a novel design of using a meandered patch with a folded end has recently been devised. The geometry of such a compact dual-frequency PIFA is shown in Figure 2.15. In this design, the meandered patch is printed on both sides of an FR4 substrate of area 10×24 mm^2, thickness 0.8 mm, and

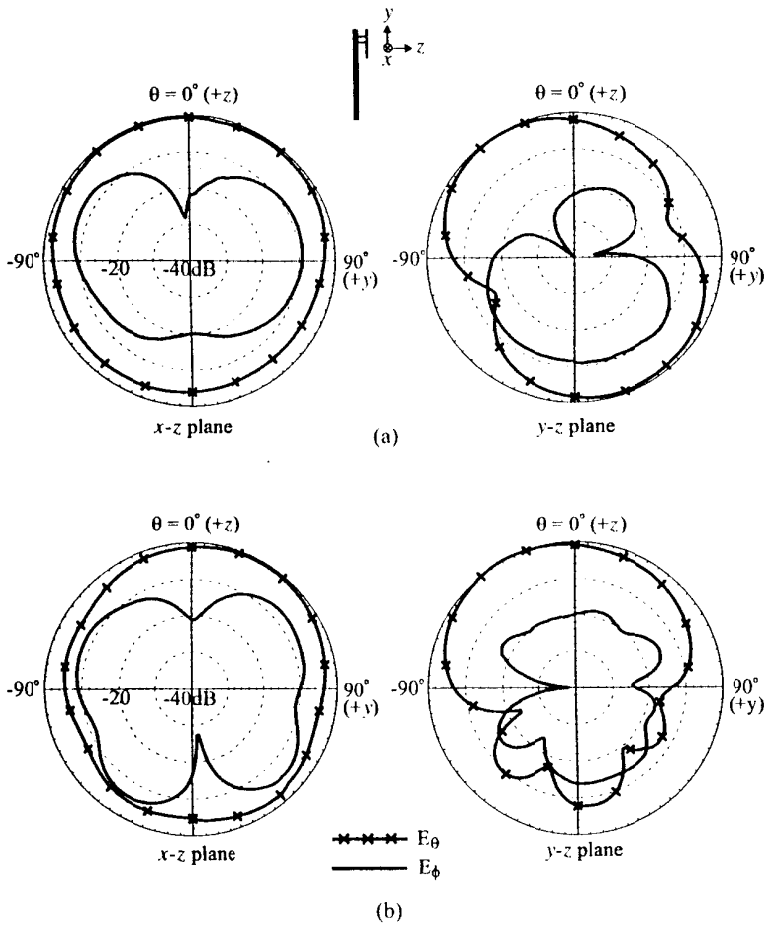

FIGURE 2.13 Measured radiation patterns at (a) 925 MHz and (b) 1795 MHz for the PIFA shown in Figure 2.11. (From Ref. 12, © 2002 IEEE, reprinted with permission)

relative permittivity 4.4. For the patch on the upper side of the FR4 substrate, two linear slits are embedded to meander the excited patch surface currents. By incorporating the patch on the lower side of the FR4 substrate, the total length of the effective patch surface current path can be much larger than the physical length of the FR4 substrate, which significantly reduces the required length of the PIFA to obtain the 900 and 1800 MHz operations.

Also note that, in this design, a rectangular notch is removed near the feed and shorting points on the patch printed on the upper side of the substrate. By varying the aspect ratio (ratio of the length and width) of this rectangular notch, the

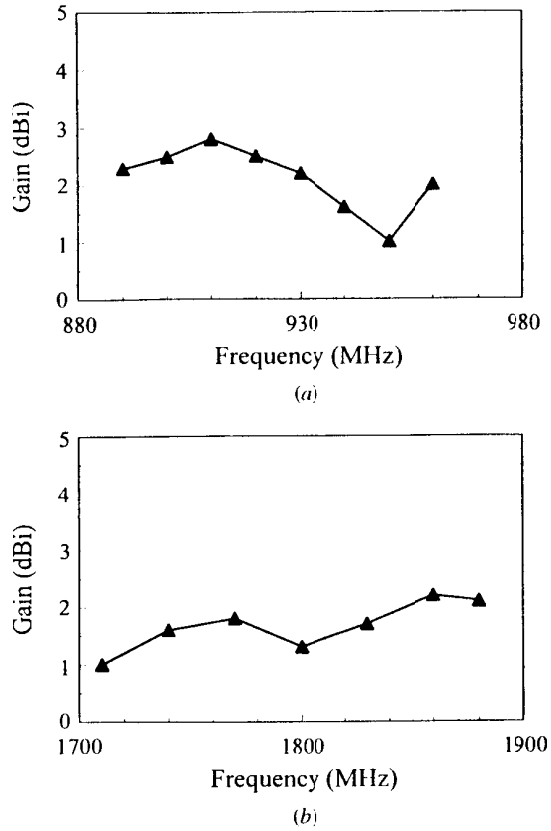

FIGURE 2.14 Measured antenna gain in (a) the GSM band and (b) the DCS band for the PIFA shown in Figure 2.11. (From Ref. 12, © 2002 IEEE, reprinted with permission)

frequency ratio of the first two resonant frequencies of the PIFA is varied in a wide range. This behavior makes the tuning of the first two resonant frequencies to be within the desired operating bands easy to achieve. A prototype of this PIFA design shown in Figure 2.15 has been successfully implemented. The prototype has an antenna height of 7.2 mm and occupies an area of $10 \times 24\ mm^2$. Measured return loss is shown in Figure 2.16. Although the constructed prototype has a compact size, the lower and upper bands still show an impedance bandwidth (2.5:1 VSWR) of about 30 and 155 MHz, respectively.

2.2.8 Patch with LC Resonators

The technique of using LC resonators to achieve dual-frequency operation has been applied to monopole antennas. This technique is also applicable for the PIFA to

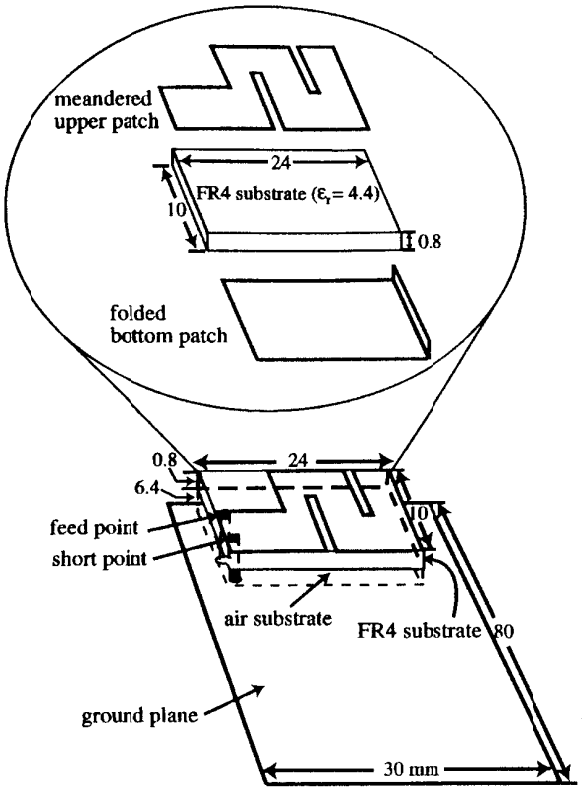

FIGURE 2.15 Geometry of the dual-frequency PIFA using a meandered patch with a folded end.

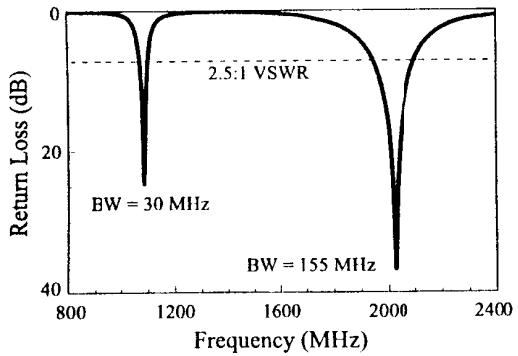

FIGURE 2.16 Measured return loss of the PIFA shown in Figure 2.15.

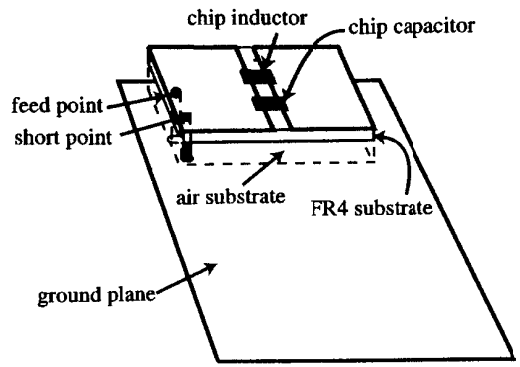

FIGURE 2.17 Geometry of the dual-frequency PIFA using a rectangular patch loaded with a chip inductor and a chip capacitor.

obtain dual-frequency operation in the 900 and 1800 MHz bands [13]. Figure 2.17 shows a typical design of the dual-frequency PIFA using a rectangular patch loaded with a chip inductor and a chip capacitor. By selecting suitable values of the chip inductor and chip capacitor, the fundamental resonant mode of the PIFA can be split into two separate resonant modes and dual-frequency operation in the 900 and 1800 MHz bands can be obtained. With a design example shown in Reference 13 using an 11-nH chip inductor and a 0.5-pF chip capacitor, the 900 and 1800 MHz dual-frequency operation has been obtained. The PIFA has a volume of about $6\times20\times30\,\text{mm}^3$, and the obtained impedance bandwidths (10 dB return loss) are about 35 and 140 MHz for the 900 and 1800 MHz bands, respectively.

2.2.9 Rectangular Spiral Strip with a Chip Inductor

Instead of using a chip inductor and a chip capacitor as described in Section 2.2.8, a simpler method of using a single chip inductor has been successfully applied to obtain dual-frequency operation of the PIFA [14]. It has been shown that, by loading a chip inductor of suitable inductance (about 12 nH or less) to the PIFA with a rectangular spiral strip (see the geometry shown in Fig. 2.18), the frequency ratio of its first two resonant frequencies can be controlled, which makes the dual-frequency operation with a desired frequency ratio easy to achieve. In addition, owing to the use of a rectangular spiral strip instead of the conventional rectangular patch, the PIFA's top patch can occupy a much reduced area for a fixed operating frequency. That is, a compact dual-frequency operation for the PIFA can be obtained.

Prototypes of the proposed dual-frequency PIFA to achieve the 900 and 1800 MHz operations have been constructed and tested. The design dimensions of the constructed prototypes, obtained with the aid of the simulation software Ansoft HFSS, are shown in Figure 2.18. The radiating element is a shorted rectangular spiral strip of constant width 2 mm and occupies an area of $10\times26\,\text{mm}^2$. The spiral

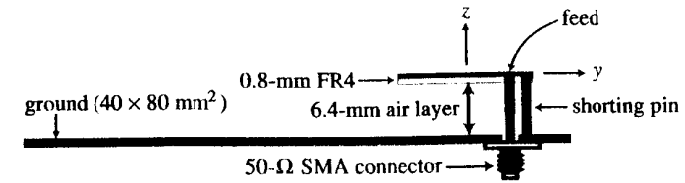

(*a*)

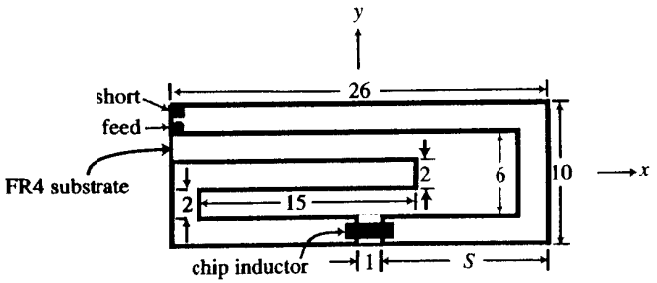

(*b*)

FIGURE 2.18 Geometry of the dual-frequency PIFA using a rectangular spiral strip with a chip inductor. (a) Side view of the PIFA mounted on the top portion of a ground plane of dimensions $40 \times 80\ \text{mm}^2$; (b) top patch of the PIFA. (From Ref. 14, © 2002 John Wiley & Sons, Inc.)

strip was printed on an FR4 substrate (thickness 0.8 mm and relative permittivity 4.4) and supported by plastic posts (not shown in the figure) of length 6.4 mm above the ground plane. Thus the total height of the proposed PIFA is 7.2 mm from the ground plane. Also note that the proposed PIFA occupies a compact area of $10 \times 26\ \text{mm}^2$.

At the outer end of the spiral strip are the feed and the shorting pin, and the total length from the open end to the inner end is about 77 mm ($= \ell_1$) in the proposed design. This length is close to one-quarter wavelength at 900 MHz, and generates a resonant mode for the lower operating frequency of the proposed dual-frequency operation. To control the upper operating frequency, a gap of 1 mm is cut in the spiral strip and a chip inductor is added as a connecting bridge across the gap. It is then found that, by varying the position of the chip inductor or the gap (S shown in Fig. 2.18b), the upper operating frequency is varied and can be controlled. In the proposed PIFA, the length from the strip's open end to the chip inductor position is about $(32 + S)$ mm ($= \ell_2$), which is also designed to be about one-quarter wavelength of the desired upper operating frequency. However, it should be noted that the inductance of the loading chip inductor also has a large effect on generating

the upper resonance of the proposed PIFA. In general, when a chip inductor of suitable inductance is used, it will perform like a short circuit for lower operating frequencies and, conversely, like an open circuit for higher operating frequencies. This behavior makes the lower and upper operating frequencies controlled, respectively, by the lengths 77 mm (the total strip length in this design) and $(32 + S)$ mm (the length from the feed to the chip inductor or the gap) in the proposed PIFA.

Figure 2.19 shows the measured and simulated return loss of the proposed PIFA with various chip inductor positions of $S = 4$, 13, and 23 mm. The loading chip

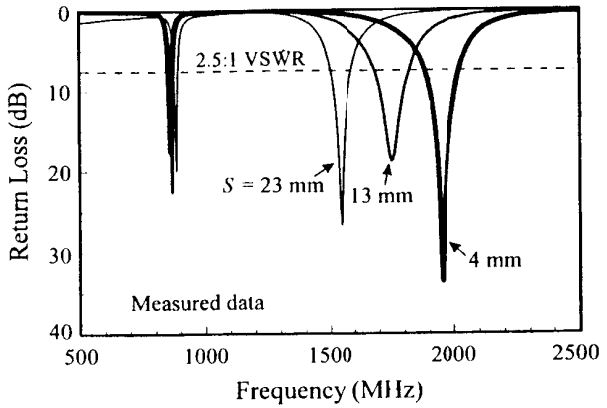

(*a*)

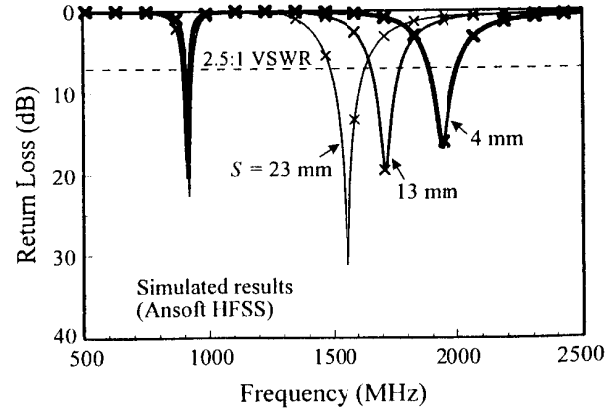

(*b*)

FIGURE 2.19 (a) Measured and (b) simulated return loss as a function of chip inductor position for the PIFA shown in Figure 2.18. (From Ref. 14, © 2002 John Wiley & Sons, Inc.)

TABLE 2.1 Performance of the Proposed Dual-band PIFA Shown in Figure 2.18 with a 12 nH Chip Inductor [14]. Impedance Bandwidth (BW) is Determined From 2.5:1 VSWR.

	S (mm)	ℓ_1 (mm)	ℓ_2 (mm)	f_1, BW (MHz, MHz)	f_2, BW (MHz, MHz)	f_2/f_1
Antenna A	4	77	36	860, 14	1952, 116	2.27
Antenna B	13	77	45	865, 14	1747, 145	2.02
Antenna C	23	77	55	884, 18	1542, 115	1.74

inductor has an inductance of 12 nH. It is first seen that the measured data in general agree with the simulated results. The measured data are also given in Table 2.1 for comparison. It is seen that the lower operating frequencies (f_1) are all close to 900 MHz, as designed, and very slight variations are observed for the three cases studied. Conversely, the upper operating frequency (f_2) decreases with an increase in S. This is because increasing the length S increases the length ℓ_2 from the feed to the gap, and thus the resonant frequency controlled by this length decreases. In this study, as S is varied from 4 to 23 mm, the obtained frequency ratios (f_2/f_1) of the two operating frequencies are in a range from about 2.27 to 1.74. Also note that antenna B ($S = 13$ mm) has a frequency ratio of about 2.0 and its upper operating frequency is close to 1800 MHz. The obtained impedance bandwidths, determined from 2.5:1 VSWR or about 7.3 dB return loss, are, respectively, 14 and 145 MHz for the lower and upper bands of antenna B.

Figures 2.20 and 2.21 plot the measured radiation patterns of antenna B at the lower and upper resonant frequencies, respectively. In the azimuthal plane (x–z plane), the radiation patterns for both operating frequencies are close to omnidirectional, especially for the 900 MHz operation. Radiation patterns at other operating frequencies across the lower and upper bands were also measured and are similar to those shown here; that is, the radiation patterns are stable across the respective operating bands. Measured antenna gain for operating frequencies across the lower and upper bands of antenna B is shown in Figure 2.22. For the lower band, the antenna gain level is about 1.3 dBi. For the upper band, the peak antenna gain is about 1.7 dBi and gain variations are less than 1 dBi across the band.

Effects of the loading chip inductors with various inductances on the performance of the proposed PIFA were also experimentally studied. Table 2.2 lists the measured lower and upper resonant frequencies for antenna B as a function of the chip inductor with various inductances. First note that the position of the loading chip inductor is fixed ($S = 13$ mm) in this study. For the case with $L = 0$, it represents the short-circuiting condition; that is, there is no gap cut in the spiral strip. The obtained results also show relatively small variations in the lower operating frequency. On the other hand, the upper operating frequency or the antenna's second resonant frequency decreases from 2222 to 1454 MHz, when the inductance L increases from 0 to 22 nH. Note that, for the case with $L = 22$ nH, although there is a resonance at 758 MHz, the obtained return loss is worse than 7.3 dB, and thus

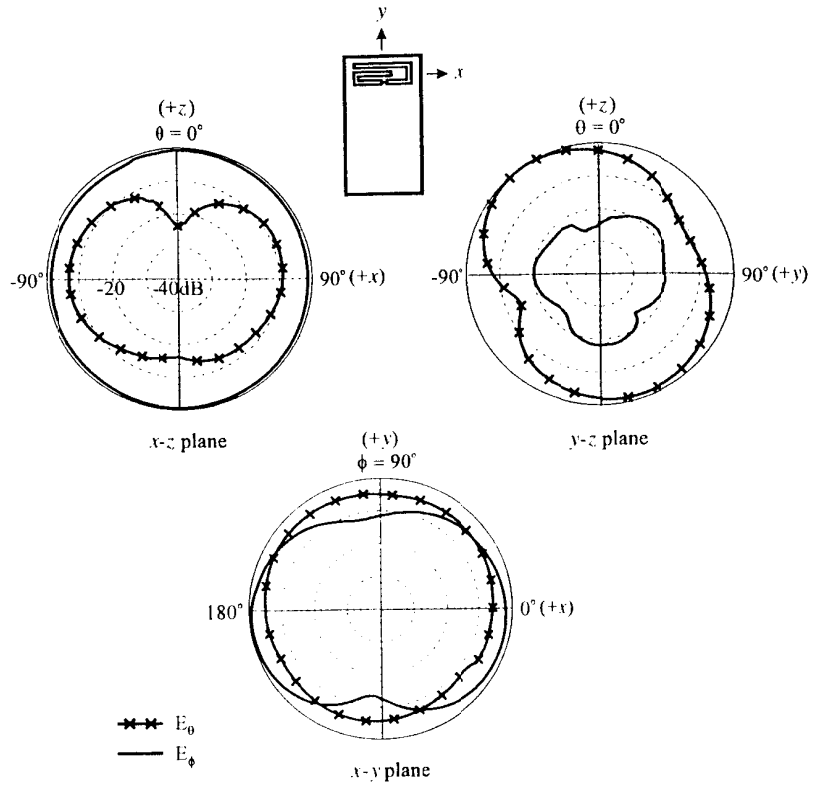

FIGURE 2.20 Measured radiation patterns at 865 MHz for the PIFA with $S = 13$ mm studied in Figure 2.19. (From Ref. 14, © 2002 John Wiley & Sons, Inc.)

no impedance bandwidth is given in Table 2.2. When L is larger than 22 nH even worse impedance matching is obtained for f_1, and the results are therefore not shown. The results obtained in Tables 2.1 and 2.2 suggest that both the position and the inductance of the loading chip inductor can effectively control the occurrence of the upper operating frequency of the proposed PIFA, with the lower operating frequency relatively very slightly affected. Thus, by suitably choosing the position and inductance of the loading chip inductor, dual-frequency operation with a wide frequency ratio range can be obtained.

2.2.10 Rectangular Spiral Strip with Nonuniform Widths

It has also been found that, by selecting different widths in different sections of a shorted rectangular spiral strip, dual-frequency operation in the 900 and 1800 MHz bands can be obtained. Figure 2.23 shows the geometry of such a

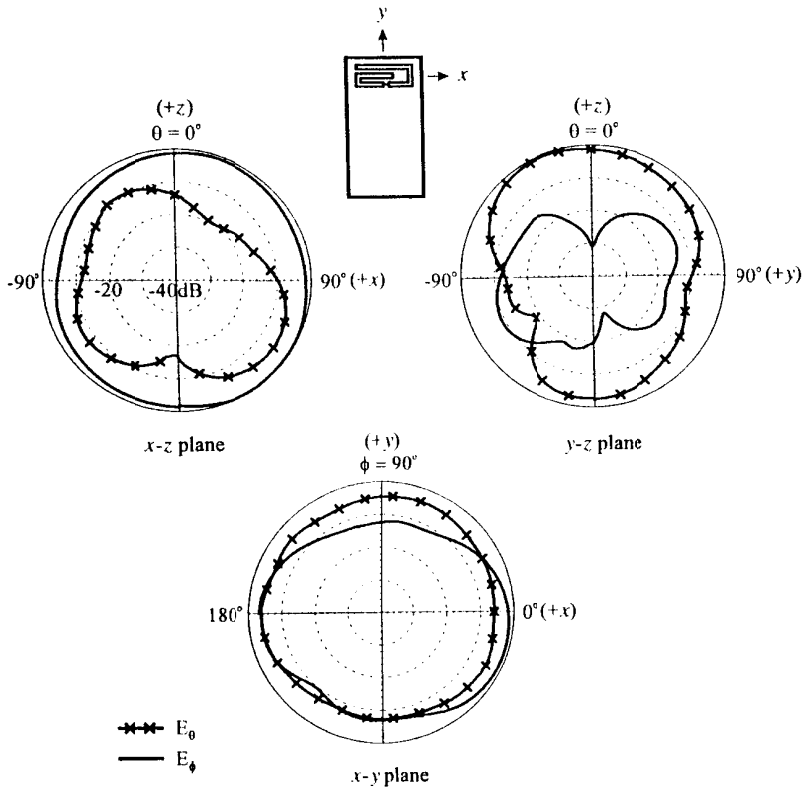

FIGURE 2.21 Measured radiation patterns at 1747 MHz for the PIFA with $S = 13$ mm studied in Figure 2.19. (From Ref. 14, © 2002 John Wiley & Sons, Inc.)

dual-frequency PIFA. The rectangular spiral strip used in this design has a structure similar to that shown in Figure 2.18, in which the strip width is a constant and dual-frequency operation is obtained by loading a chip inductor. In this design, however, the strip width is nonuniform, and each straight section (there are 6 straight sections in the design shown in Fig. 2.23) of the rectangular spiral strip has different strip widths. In general, to achieve better impedance bandwidth, it is preferred that the strip width increases from the first straight section at the outer open end, where the feed and shorting points are located, to the last straight section having the inner surrounded open end.

Also note that the two operating frequencies in this design utilize the first two resonant frequencies of the PIFA, which share a common resonant path starting from the feed point near the strip's outer open end to the strip's inner surrounded open end. In addition, the total length of the shorted rectangular spiral strip can be approximately determined from one-quarter wavelength of the lower frequency

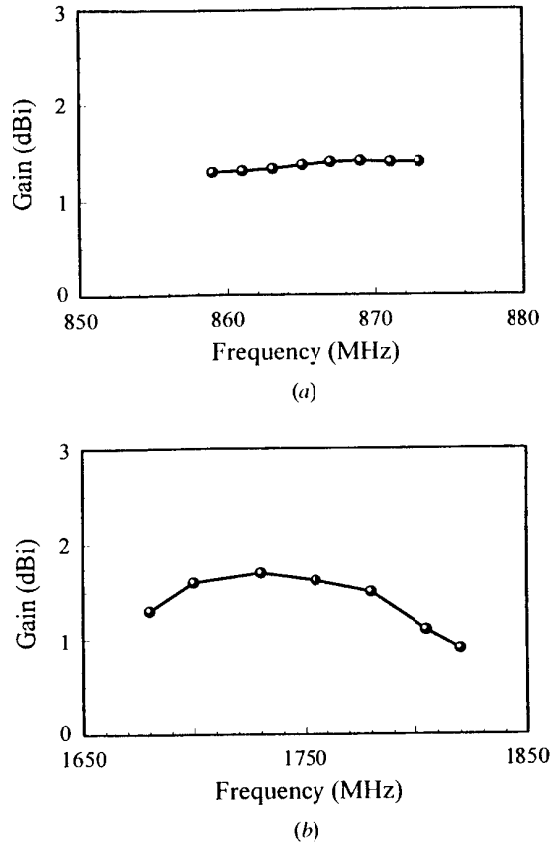

FIGURE 2.22 Measured antenna gain across (a) the lower band and (b) the upper band of the PIFA studied in Figure 2.19. (From Ref. 14, © 2002 John Wiley & Sons, Inc.)

TABLE 2.2 Performance of Antenna B Shown in Table 2.1 with Various Chip Inductors [14].

L (nH)	f_1, BW (MHz, MHz)	f_2, BW (MHz, MHz)	f_2/f_1
0(short-circuit)	992, 20	2222, 112	2.24
1.5	980, 22	2138, 116	2.18
3.3	962, 18	2048, 112	2.13
6.8	914, 18	1910, 128	2.09
12	865, 14	1747, 145	2.02
22	758, —	1454, 94	1.92

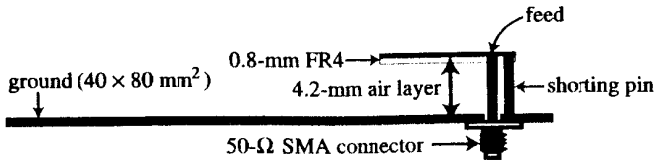

(*a*)

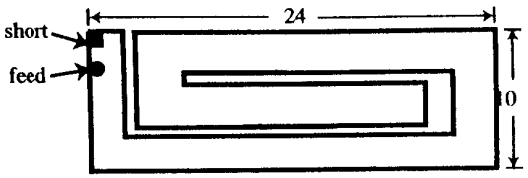

(*b*)

FIGURE 2.23 Geometry of the dual-frequency PIFA using a rectangular spiral strip of nonuniform widths. (a) Side view of the PIFA mounted on the top portion of a ground plane of dimensions $40 \times 80\,\text{mm}^2$; (b) top patch of the PIFA.

(900 MHz in this design) of the desired dual-frequency operation. A prototype of the proposed PIFA for 900 and 1800 MHz dual-frequency operations has also been implemented and tested. The constructed prototype has a height of 5 mm and occupies an area of only $10 \times 24\,\text{mm}^2$. Figure 2.24 shows the measured and simulated return loss. Reasonable agreement of the measurement and the simulation is obtained, and two separate resonant modes near 900 and 1800 MHz are successfully excited. Because the constructed prototype has compact dimensions ($5 \times 10 \times 24\,\text{mm}^3$), the proposed PIFA design is a very attractive candidate for practical applications in mobile phones that have a very limited realty space for the antenna.

2.3 TRIPLE-FREQUENCY PIFA

2.3.1 Two or Three Separate Patches

Figure 2.25 shows two promising configurations of the top patch of the triple-frequency PIFA for the 900, 1800, and 2450 MHz operations. In Figure 2.25a, the top patch comprises three separate shorted patches with a triple feed; patch 1 is

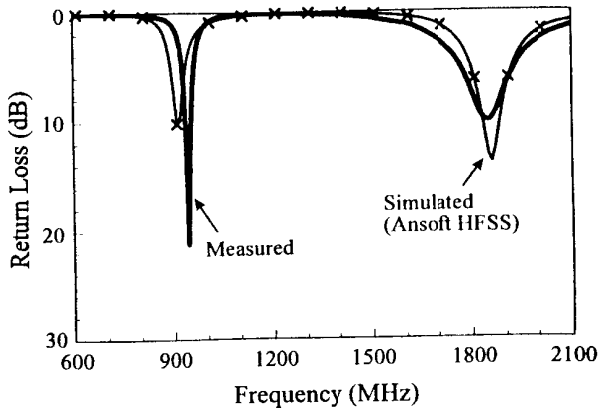

FIGURE 2.24 Measured and simulated return loss of the PIFA shown in Figure 2.23.

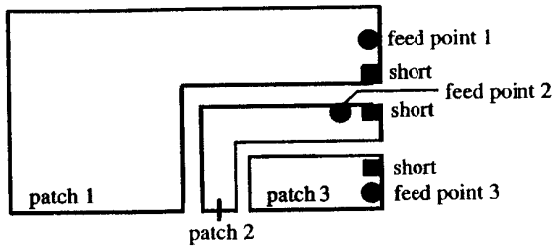

(*a*)

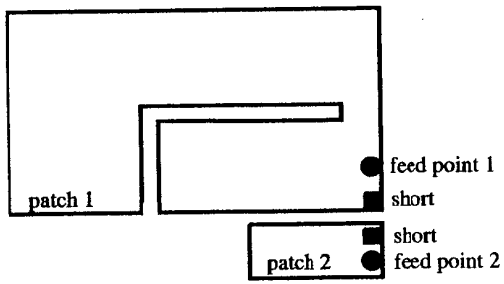

(*b*)

FIGURE 2.25 Top patch of the triple-frequency PIFA comprising (a) three separate patches with a triple feed and (b) two separate patches with a dual feed for achieving 900, 1800, and 2450 MHz operations.

for GSM operation in the 900 MHz band, patch 2 is for DCS operation in the 1800 MHz band, and patch 3 is for WLAN operation in the 2450 MHz band. Notice that these three patches are arranged in a compact configuration and have separate shorting and feed points. These three patches are all operated as quarter-wavelength resonant structures. Such a PIFA design with a triple feed can find applications where mobile phones require separate feeds for operations in GSM, DCS, and WLAN bands.

For the configuration shown in Figure 2.25b, the top patch consists of two separate patches, with the larger patch (patch 1 in the figure) loaded with an L-shaped slit for GSM and DCS dual-frequency operations (see the discussion in Section 2.2.2). In this design, the smaller patch (patch 2) is for WLAN operation in the 2045 MHz band and is also operated as a quarter-wavelength resonant structure. The two patches utilize different shorting and feed points, and such a design is suitable for mobile phones using the same feed for GSM and DCS operations and a second feed for WLAN operation.

2.3.2 A Meandered Patch

By using a meandered patch, a triple-frequency PIFA for operations in the 900, 1800, and 2450 MHz bands can also be obtained. A promising geometry is shown in Figure 2.26. In this design, instead of the triple-feed and dual-feed designs shown in Section 2.3.1, triple-frequency operation can be achieved by using a single feed. A related PIFA design, in which two linear slits are embedded in the top patch to meander the excited patch surface current paths, has been reported in Reference 16. This meandering can lead to a compact size for the PIFA and can also strongly affect the first three resonant frequencies of the PIFA. Thus, by choosing proper dimensions of the two linear slits, the PIFA's first three resonant frequencies can be adjusted to be about 900, 1800, and 2450 MHz, respectively. Also note that, to

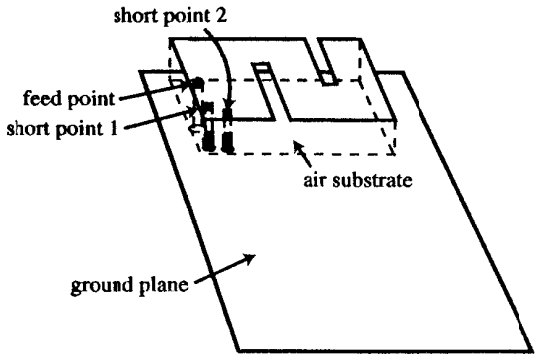

FIGURE 2.26 Geometry of the triple-frequency PIFA with a meandered patch for achieving 900, 1800, and 2450 MHz operations.

achieve good impedance matching of the three excited resonant modes, the use of two shorting pins, instead of only one, is suggested [16].

2.3.3 A Branch Line Strip with a Folded End

Recently, a triple-frequency PIFA with two shorted branch strips sharing a common shorting point and having a same feed point has been devised [17]. The geometry of this PIFA mounted on the top portion of a ground plane of dimensions $30 \times 80\ mm^2$ is shown in Figure 2.27. The PIFA consists of two shorted branch strips: the longer one (strip 1) controls the excitation of the resonant frequencies at about 900 and 1800 MHz, and the shorter one (strip 2) controls the excitation of the resonant

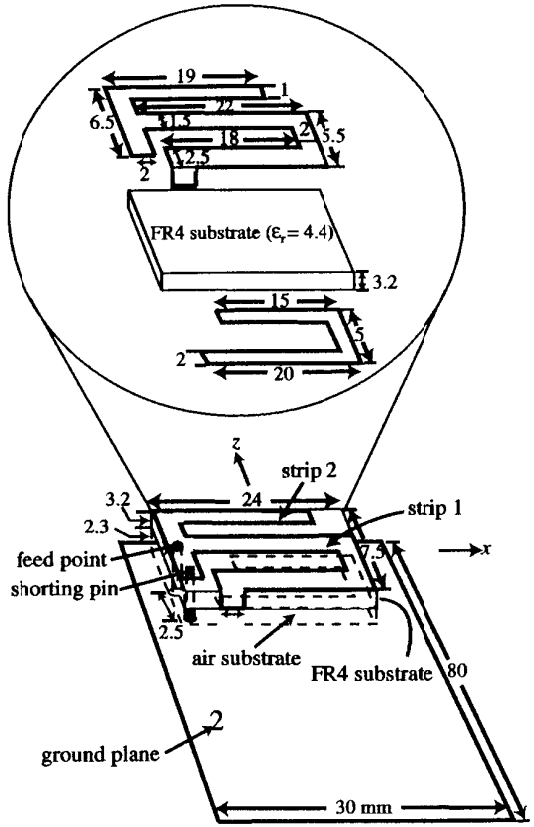

FIGURE 2.27 Geometry of the triple-frequency PIFA using a branch line strip with a folded end to achieve 900, 1800, and 2450 MHz operations. (From Ref. 17, © 2002 John Wiley & Sons, Inc.)

frequency at about 2450 MHz. The two branch strips are printed on an FR4 substrate of thickness 3.2 mm, area $7.5 \times 24\ mm^2$, and relative permittivity 4.4. Between the FR4 substrate and the ground plane is an air substrate of thickness 2.3 mm (plastic posts for supporting the FR4 substrate above the ground plane are not shown in the figure), which makes the total antenna height from the ground plane 5.5 mm. That is, the total antenna volume is $5.5 \times 7.5 \times 24\ mm^3$ or only about $1\ cm^3$. The design dimensions shown in the figure were obtained with the aid of the commercially available simulation software Ansoft HFSS.

Note that the shorter strip has a length of 24 mm (starting from the shorting pin), which corresponds to about 20% of the wavelength at 2450 MHz. This length is less than one-quarter wavelength, and this behavior is largely due to the effect of the thick FR4 substrate used, which results in a larger effective relative permittivity of the combined FR4 and air substrates between the shorted strip and the ground plane. The longer strip has a length of about 87 mm, corresponding to about 26% of the wavelength at 900 MHz. Note that the longer strip is meandered and printed on both sides of the FR4 substrate, which effectively reduces the PIFA. However, probably because of the meandering, which increases the possible coupling between two adjacent meandered sections, the effective strip length is decreased; that is, a larger strip length is required for operating at a fixed frequency. This is probably the reason that the strip length in operating wavelength is larger for the longer strip than for the shorter strip.

Also note that the proposed PIFA operates at the first resonant frequency of the shorted strip and the first two resonant frequencies of the longer strip. Because only one resonant frequency is required for the shorter strip, the adjusting of this resonant frequency to be the desired one can be easily achieved by fine-tuning the length of the shorter strip. On the other hand, to adjust the first two resonant frequencies to the desired frequencies, the widths of each meandered sections of the longer strip (see the design dimensions given in Fig. 2.27) are chosen to be different values, which are very effective in adjusting the frequency ratio of the longer strip's first two resonant frequencies.

A prototype based on the design dimensions shown was constructed and studied. Figure 2.28 shows the measured and simulated return loss of the constructed prototype. Very good agreement between the measured data and the simulated results is seen. Three resonant frequencies close to 900, 1800, and 2450 MHz are excited with good impedance matching. With respect to their respective center frequency, the three frequency bands, determined from 2.5:1 VSWR or about 7.3 dB return loss, have impedance bandwidths of about 18 MHz (about 1.9%), 85 MHz (about 4.8%), and 70 MHz (about 2.9%), respectively. Note that, although the proposed PIFA occupies a much smaller volume (less than 10%) than that in References 15 and 16, no large decreases in the obtained impedance bandwidths are seen.

The radiation characteristics were also studied. Figures 2.29–2.31 plot the measured radiation patterns at the center frequency of the three frequency bands. For 950 MHz (Fig. 2.29), the measured radiation pattern in the azimuthal plane (x–y plane) is close to omnidirectional radiation and the measured antenna gain is

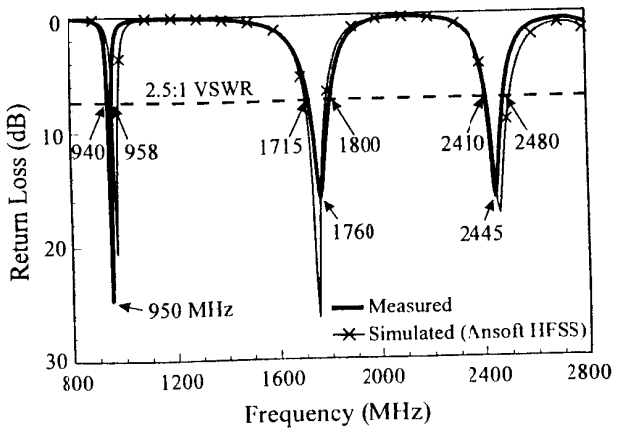

FIGURE 2.28 Measured and simulated return loss for the PIFA shown in Figure 2.27. (From Ref. 17, © 2002 John Wiley & Sons, Inc.)

about 0 dBi. For 1760 MHz (Fig. 2.30), the measured radiation pattern in the azimuthal plane (x–y plane) is less close to omnidirectional radiation than that for 950 MHz. However, the measured antenna gain is higher and is about 2.2 dBi. In the elevation plane of y–z plane, the forward radiation ($-y$ direction) is seen to be much greater than the backward radiation ($+y$ direction or behind the ground plane). The measured radiation patterns for 2450 MHz are plotted in Figure 2.31, and the measured antenna gain is about 1.5 dBi. Also note that the radiation characteristics of the operating frequencies across each frequency band were also measured, and the radiation patterns are stable in each frequency band.

2.4 PIFA WITH AN L-SHAPED GROUND

2.4.1 Patch PIFA Design

Instead of using a simple flat ground plane, a PIFA with an L-shaped ground plane has also been studied. It has been found that such a PIFA can have decreased backward radiation and enhanced antenna gain. A related study is reported in Reference 18. Figure 2.32a shows the geometry of a conventional PIFA with a simple flat ground plane for an internal mobile phone antenna, and the proposed PIFA with an L-shaped ground plane is presented in Figure 2.32b. In both geometries, the simple flat ground plane in Figure 2.32a and the horizontal ground plane in Figure 2.32b have the same dimensions of $60 \times 40\ mm^2$. An additional vertical ground is added to the edge of the horizontal ground plane in the proposed design to enhance the antenna performance. In this case, the vertical ground and the horizontal ground plane form an L-shaped ground plane for the proposed design.

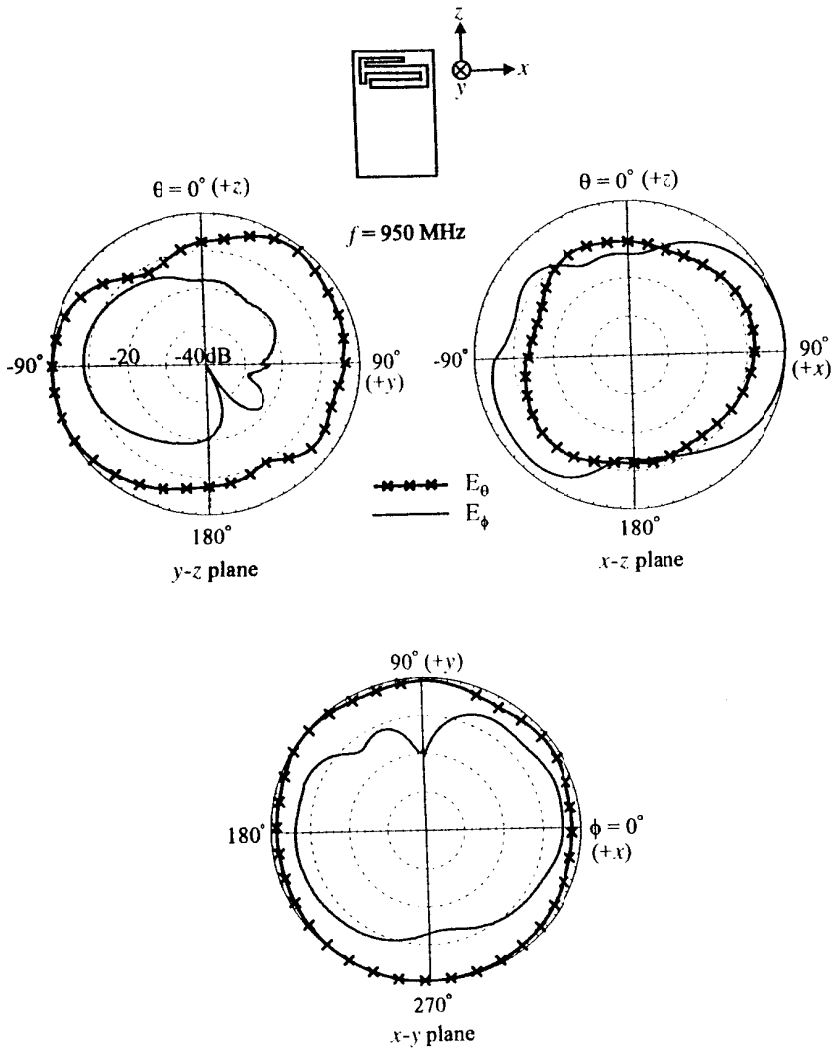

FIGURE 2.29 Measured radiation patterns at 950 MHz for the PIFA studied in Figure 2.28. (From Ref. 17, © 2002 John Wiley & Sons, Inc.)

In addition, because of the additional vertical ground, the coax feed can be placed in the same plane as the radiating patch as seen in Figure 2.32b or below the horizontal ground plane as seen in Figure 2.32a, which gives the proposed design flexible feed arrangements.

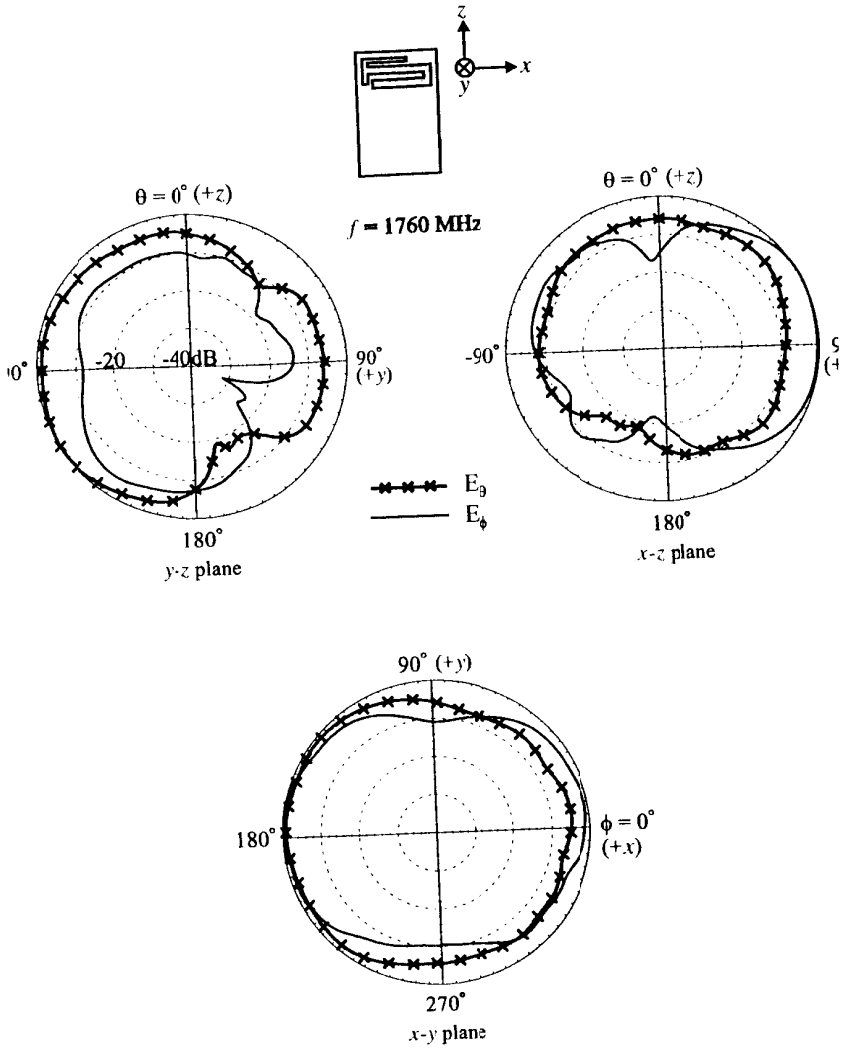

FIGURE 2.30 Measured radiation patterns at 1760 MHz for the PIFA studied in Figure 2.28. (From Ref. 17, © 2002 John Wiley & Sons, Inc.)

It should be noted that the dimensions given in Figure 2.32b are for achieving UMTS band operation. The PIFA is fed at the center of the edge of the top patch, which has dimensions $30 \times 15\,\text{mm}^2$ and is placed above the horizontal ground plane with a height of 7 mm. The top patch is also placed close to the vertical ground to reduce the required probe pin length of the coplanar coax feed, which makes

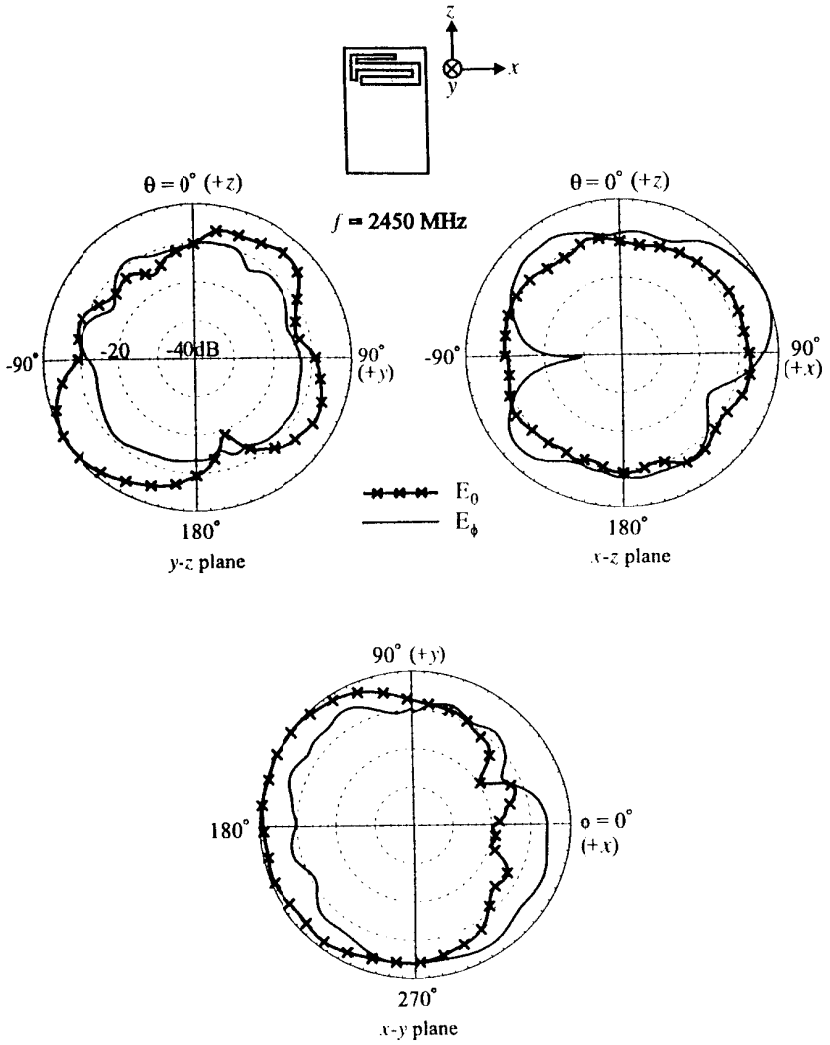

FIGURE 2.31 Measured radiation patterns at 2450 MHz for the PIFA studied in Figure 2.28. (From Ref. 17, © 2002 John Wiley & Sons, Inc.)

impedance matching of the proposed PIFA over a wide bandwidth easy to achieve. In this design, the distance between the vertical ground and the patch edge is 2 mm and the shorting point is 1 mm away from the feed point. Also note that, for the corresponding conventional PIFA shown in Figure 2.32a, all the dimensions are

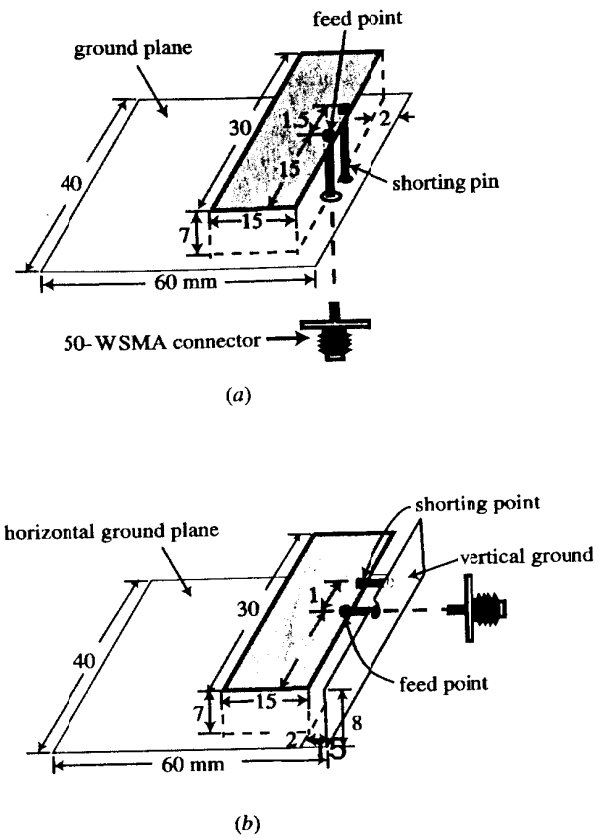

FIGURE 2.32 Geometries of the PIFA with (a) a simple ground plane (reference 1) and (b) an L-shaped ground plane. (From Ref. 18, © 2002 John Wiley & Sons, Inc.)

the same as those given in Figure 2.32b except that the distance between the shorting point and the feed point is 1.5 mm to achieve good impedance matching.

Figure 2.33 shows the measured and simulated return loss for the corresponding conventional PIFA (references 1 and 2) and the proposed PIFA. Good agreement between the measurement and the simulation for references 1 and 2 shown in Figure 2.33a is obtained. For the results of the proposed PIFA in Figure 2.33b, reasonable agreement between the measured data and the simulated results is also obtained. It is seen that the proposed PIFA has a wide impedance bandwidth (10 dB return loss) of 310 MHz (1920–2230 MHz), which covers the required operating bandwidth of the UMTS band. It should also be noted that, although the patch size is the same, the obtained bandwidth of the proposed PIFA has higher frequencies than those of the corresponding conventional design of reference 1. By decreasing the patch

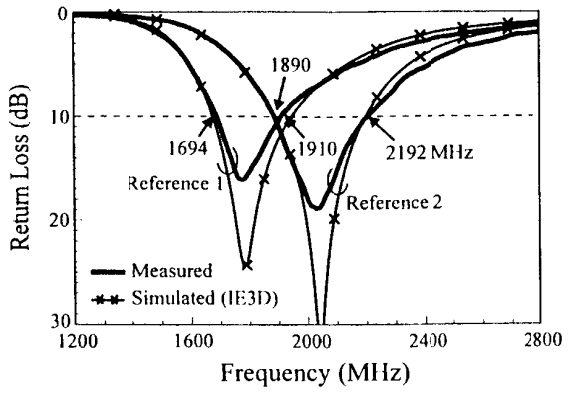

(*a*)

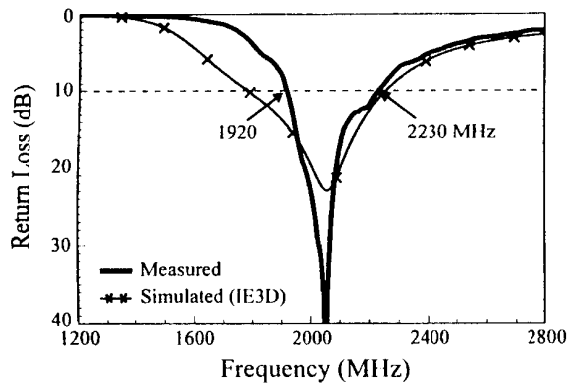

(*b*)

FIGURE 2.33 Measured and simulated return loss against frequency. (a) The conventional design [reference 1: patch size $15\times30\,mm^2$ as shown in Figure 2.32a; reference 2: patch size $13\times26\,mm^2$; other parameters for both references 1 and 2 are the same and are given in Figure 2.32a]; (b) the proposed design with an L-shaped ground plane [dimensions given in Figure 2.32b]. (From Ref. 18, © 2002 John Wiley & Sons, Inc.)

size from $15\times30\,mm^2$ to $13\times26\,mm^2$, the conventional design of reference 2 has an operating bandwidth at frequencies about the same as those of the proposed PIFA.

Figure 2.34 shows the measured radiation patterns for references 1 and 2 at resonance. No prominent difference in the radiation patterns is observed, although references 1 and 2 have different ground plane size in wavelength. However, with comparison to the measured radiation patterns of the proposed design shown in Figure 2.35, it is clearly seen that, in the azimuthal plane (x–y plane), the backward

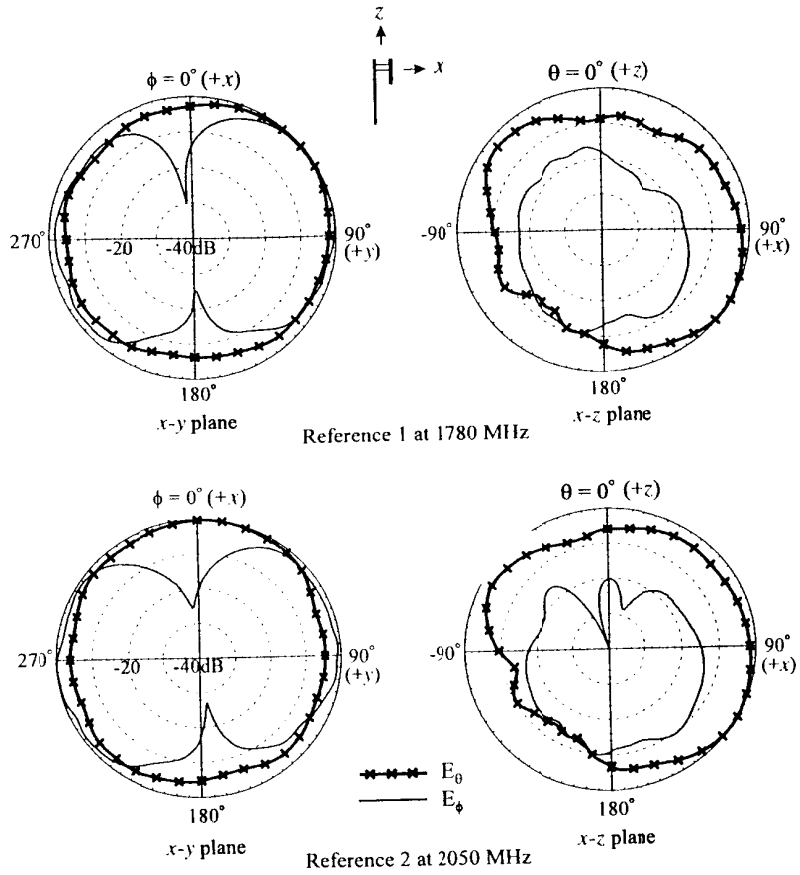

FIGURE 2.34 Measured radiation patterns at resonance for the reference PIFAs studied in Figure 2.33. (From Ref. 18, © 2002 John Wiley & Sons, Inc.)

radiation in the direction of $\varphi = 180°$ is smaller for the proposed PIFA than for the conventional PIFA. For the vertical plane (x–z plane), it is also observed that the radiation behind the ground plane is much smaller for the proposed PIFA than for the conventional PIFA. Figure 2.36 also shows the measured antenna gain for frequencies within the operating bandwidths for the reference PIFAs and the proposed PIFA. References 1 and 2 show about the same antenna gain level, which is lower than that of the proposed PIFA by about 1 dBi. The proposed PIFA has a peak antenna gain of about 3.5 dBi, and the gain variations are within 1.2 dBi for frequencies within the UMTS band.

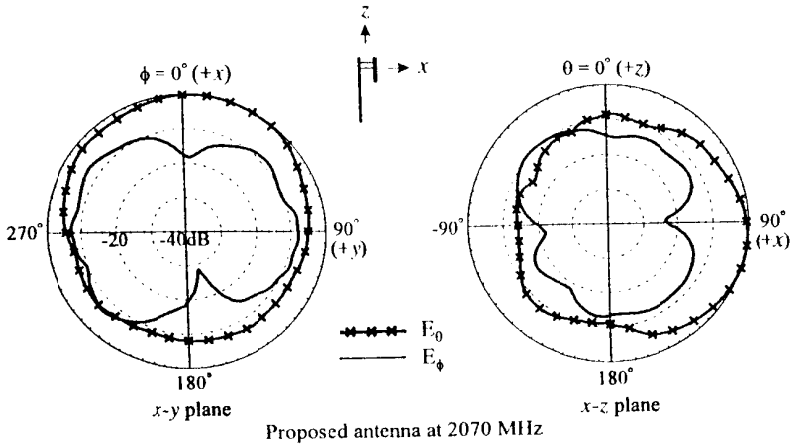

FIGURE 2.35 Measured radiation patterns at resonance for the proposed PIFA studied in Figure 2.33. (From Ref. 18, © 2002 John Wiley & Sons, Inc.)

2.4.2 Wire PIFA Design

A wire PIFA with an L-shaped ground plane has also been studied. A prototype of such a PIFA mounted on the top portion of a UMTS mobile phone ground plane is shown in Figure 2.37. The dimensions given in the figure are for achieving UMTS operation in the 2050 MHz band. The wire PIFA was constructed by using conducting wires with a diameter of 1 mm, and there are three sections in this wire PIFA: one shorting arm, one feed arm, and an inverted-L wire and an L-shaped ground plane comprising a vertical ground and a horizontal ground. The vertical ground, with dimensions $15 \times 30\ mm^2$, is for reducing the PIFA's backward radiation toward the user's head and the horizontal ground, with dimensions $10 \times 30\ mm^2$, can reduce the PIFA's radiation toward the associated microwave circuitry of the mobile phone, thereby reducing the electromagnetic interference and enhancing the system performance.

The shorting arm has a length of 9 mm and short-circuits the wire PIFA to the vertical ground. This arrangement can achieve enhanced impedance matching for the proposed wire PIFA. The feed arm has a length of 10 mm and is connected to the feed through a via-hole in the horizontal ground. The inverted-L wire has a total length of 30 mm, and its open end is bent to reduce its linear dimension to 25 mm. Note that it is possible, by further bending the open end of the inverted-L wire toward the feed arm, to obtain a much smaller linear dimension.

A prototype based on the design dimensions given in Figure 2.37 has been constructed and tested. Figure 2.38 shows the measured and simulated return loss for the prototype. A resonant mode is excited with good impedance matching at about 2 GHz, and excellent agreement between the measurement and the simulation is observed. However, the obtained impedance bandwidth (2.5:1 VSWR) is about

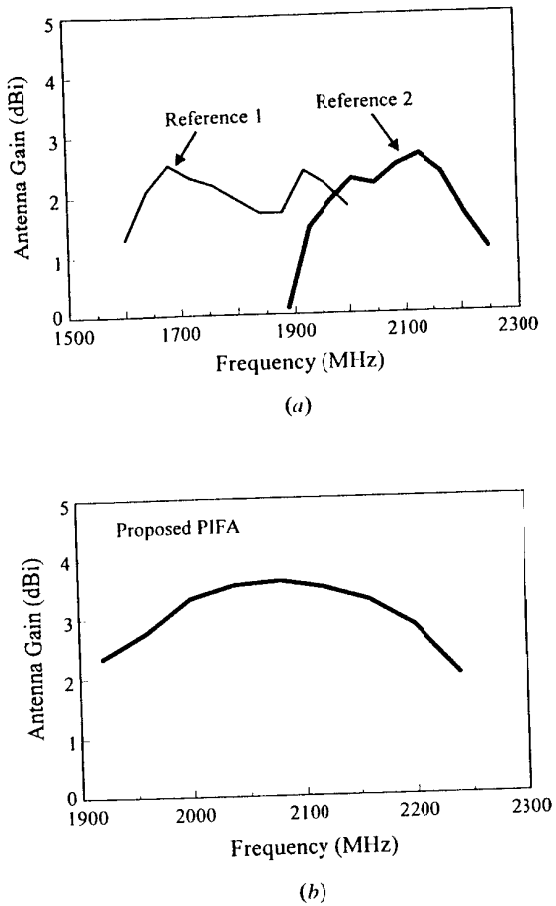

FIGURE 2.36 Measured antenna gain for (a) the reference PIFAs and (b) the proposed PIFA studied in Figure 2.33. (From Ref. 18, © 2002 John Wiley & Sons, Inc.)

150 MHz only, and wider impedance bandwidth is required for UMTS operation (250 MHz). Measured radiation patterns at 2000 MHz are also plotted in Figure 2.39. In the elevation plane (x–z plane), it is clearly seen that the forward radiation is much larger than the backward radiation, and the radiation in the upper half plane is lower than that in the lower half plane. In addition, the E_θ and E_φ components are comparable in the three principal planes, which can provide polarization diversity for mobile phones and is an advantage for wireless communications where their wave propagation environment is complex. In this case, the effect of the multipath fading problem is decreased and the system performance can be enhanced. Antenna gain

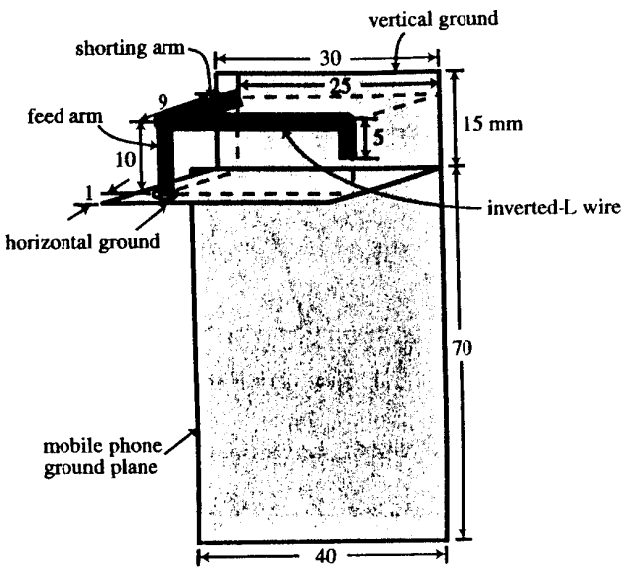

FIGURE 2.37 Geometry of the wire PIFA with an L-shaped ground plane for a UMTS mobile phone.

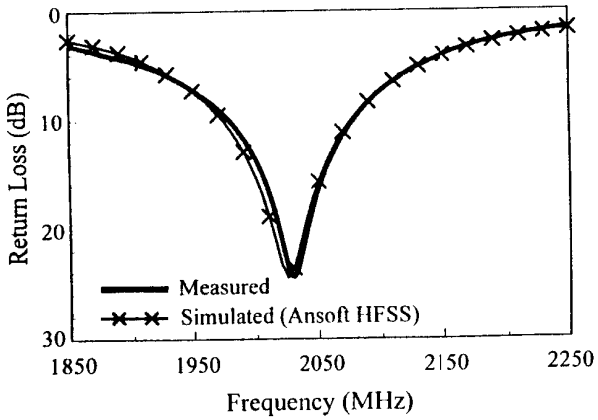

FIGURE 2.38 Measured and simulated return loss for the PIFA shown in Figure 2.37.

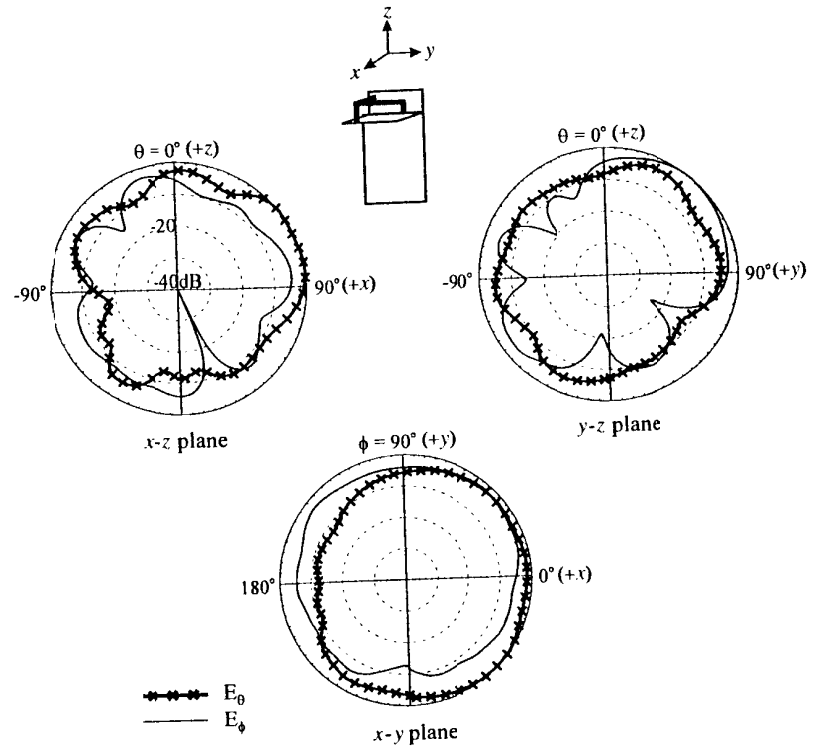

FIGURE 2.39 Measured radiation patterns at 2000 MHz for the PIFA shown in Figure 2.37.

for the constructed prototype was also measured, and a gain level of about 2.5 dBi is obtained.

2.5 STACKED PIFA

By stacking two PIFAs, enhanced impedance bandwidth can be obtained for a fixed antenna volume [19, 20]. This design method is very attractive for applications where realty space is very limited but wide operating bandwidth for the antenna is required. The bandwidth enhancement for this kind of stacked PIFAs is obtained by adjusting the lengths of the two stacked shorted patches to be slightly different, which makes it possible for the excitation of two resonant modes at close frequencies, thereby leading to a wider impedance bandwidth formed by the two closely excited resonant modes.

Figure 2.40 shows the geometry of a stacked PIFA for DCS operation in the 1800 MHz band. To be suitable as a surface mountable device, the lower patch is

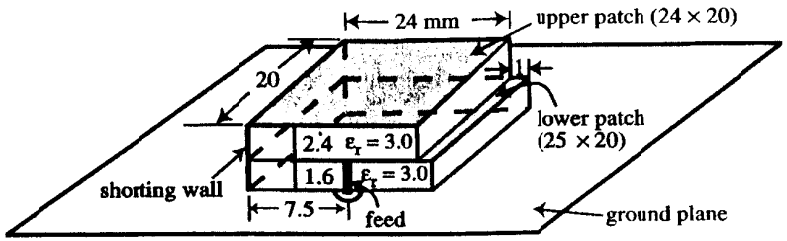

FIGURE 2.40 Geometry of a stacked PIFA for DCS operation in the 1800 MHz band. (From Ref. 20, © 2001 IEEE, reprinted with permission)

directly fed by a probe feed at the patch edge and the upper patch is parasitically coupled from the lower patch. Both patches have a common shorting wall and are printed on a low-loss dielectric substrate of relative permittivity 3.0. The substrate thicknesses for the upper and lower patches are 2.4 and 1.6 mm, respectively; that is, the total antenna height is only 4 mm. The length of the lower patch is 25 mm, whereas that of the upper patch is 24 mm. The feed point is 7.5 mm away from the common shorting wall. Figure 2.41 shows the measured return loss for the design shown in Figure 2.40. It is clearly seen that two resonant modes are excited at close frequencies, and the impedance bandwidth, determined from 10 dB return loss, reaches 202 MHz (1688–1890 MHz) or about 11.2% referenced to 1800 MHz. The obtained bandwidth covers the required bandwidth of the GSM system and is estimated to be about 1.5 times that of a single-layer PIFA occupying the same physical volume.

Figure 2.42 shows a design example of the stacked PIFA for GSM operation in the 900 MHz band. In this design, the lengths of the lower and upper patches are

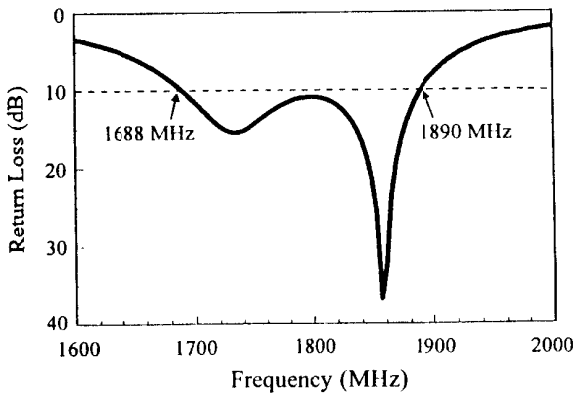

FIGURE 2.41 Measured return loss for the PIFA shown in Figure 2.40. (From Ref. 20, © 2001 IEEE, reprinted with permission)

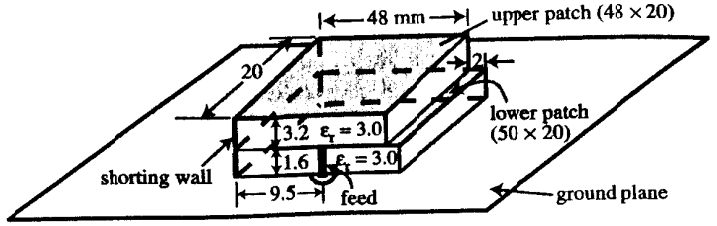

FIGURE 2.42 Geometry of the stacked PIFA for GSM operation in the 900 MHz band. (From Ref. 20, © 2001 IEEE, reprinted with permission)

adjusted to be 50 and 48 mm, respectively. The substrate thickness of the upper patch is also increased to be 3.2 mm, and the feed point is at a distance of 9.5 mm from the common shorting wall. Other design parameters are the same as described in Figure 2.40 for DCS operation. Measured return loss is shown in Figure 2.43, and the obtained impedance bandwidth reaches 94 MHz (868–962 MHz) or about 10.4% referenced to 900 MHz, which covers the required bandwidth of the GSM system. The obtained bandwidth is also about 1.5 times that of a single-layer PIFA occupying the same physical volume.

2.6 GROUND PLANE EFFECT ON IMPEDANCE BANDWIDTH OF THE PIFA

Effects of the ground plane dimensions on the impedance bandwidth of the PIFA have been studied, and it has been found that, by varying either the ground plane

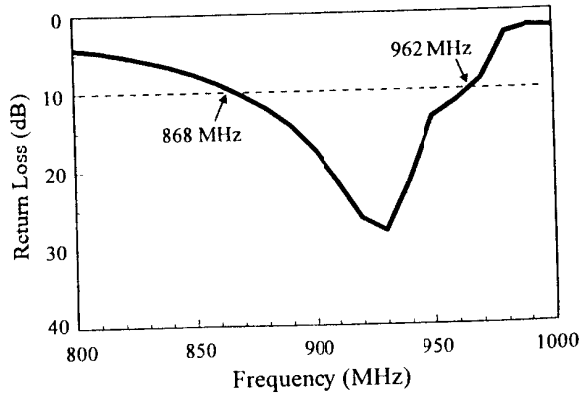

FIGURE 2.43 Measured return loss for the PIFA shown in Figure 2.42. (From Ref. 20, © 2001 IEEE, reprinted with permission)

length or width, the PIFA's impedance bandwidth can be significantly varied [21]. The bandwidth variations are larger than 300 MHz for the PIFA with a center operating frequency designed at about 2 GHz for a UMTS mobile phone, and there exists an optimal ground-plane length for obtaining maximum impedance bandwidth. In addition, there is a critical value for the ground plane width. When the ground plane width is less than the critical value, relatively very sharp variations in the impedance bandwidth have been observed.

Figure 2.44 shows the geometry of the PIFA mounted on the top portion of a ground plane of length L and width W. For applications in the UMTS band, whose center frequency is at 2050 MHz and whose required bandwidth is 250 MHz, the PIFA was chosen to have a length 24 mm and a width 18 mm and has an air-layer substrate of thickness 6.4 mm; that is, the PIFA occupies a volume of $24 \times 18 \times 6.4$ mm^3. To excite the antenna, a probe feed is placed at the center of the top patch (it can also be at the edge of the top patch), which is short-circuited to the ground plane with a shorting pin placed close to the feed point with a distance of d. It should be noted that, to achieve optimal impedance matching for the PIFA with

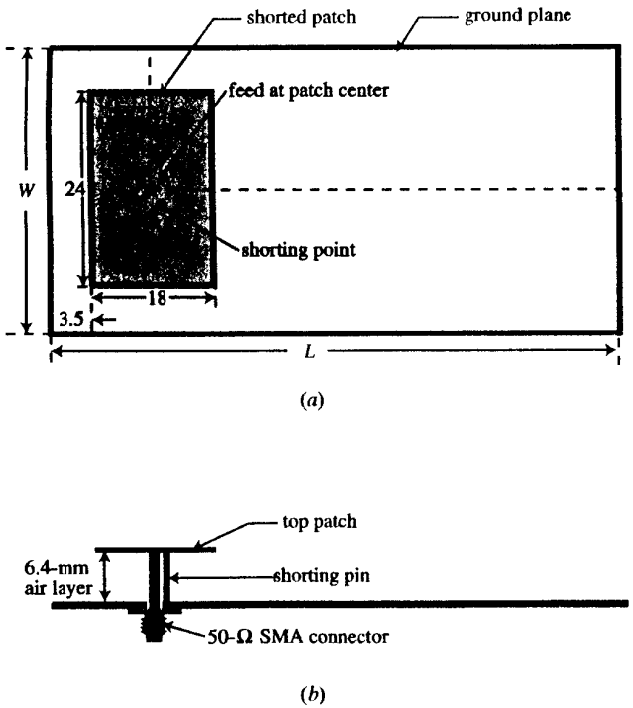

FIGURE 2.44 Geometry of the PIFA with a simple rectangular top patch for a UMTS mobile phone. (a) Top view; (b) side view. (From Ref. 21, © 2002 John Wiley & Sons, Inc.)

various ground plane dimensions, the distance d was not fixed and was slightly varied from about 0.75 to 2 mm in the experiment.

The PIFA shown in Figure 2.44 with various ground plane lengths and widths was studied experimentally. In the study the ground plane width was first fixed to be 30 mm, and Figure 2.45 shows the measured return loss against frequency for the PIFA with various ground plane lengths of 65–90 mm. It is clearly seen that the measured return loss is significantly affected by the variation in the ground plane length. The obtained impedance bandwidth, determined by 10 dB return loss, and the center operating frequency, defined to be the average of the lower and higher frequencies with 10 dB return loss, as a function of the possible ground plane length for a mobile phone are presented in Figure 2.46. It is observed that, for L varying from 50 to 105 mm, the obtained impedance bandwidths vary from about 150 to 490 MHz, a variation of over 300%. The optimal impedance bandwidth occurs at about $L = 65$ mm, which corresponds with about 45% of the free space wavelength at 2050 MHz, the center frequency of the UMTS band. It should also be noted that, for cases with $L = 51$–83 mm, the obtained impedance bandwidths are all greater than 250 MHz, the required bandwidth for UMTS operation. As for the center operating frequency shown in Figure 2.46b, the variations in the ground plane length also cause a variation of about 70 MHz, from about 2045 to 2115 MHz.

Effects of various ground plane widths on the measured impedance bandwidth and the center operating frequency have also been studied. Figure 2.47 shows the results for the case with the ground plane length fixed at 65 mm, which is the optimal length in the study shown in Figure 2.46. Measured results show that both the impedance bandwidth and the center operating frequency increase monotonically with decreasing ground plane width, which is quite different from the results of the ground plane length variations observed in Figure 2.46. It is also seen that,

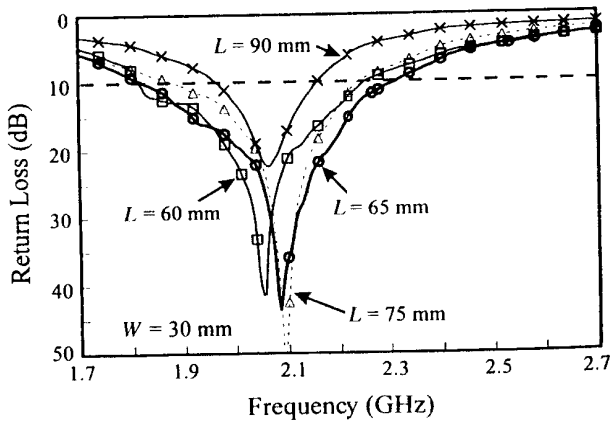

FIGURE 2.45 Measured return loss for the PIFA shown in Figure 2.44. (From Ref. 21, © 2002 John Wiley & Sons, Inc.)

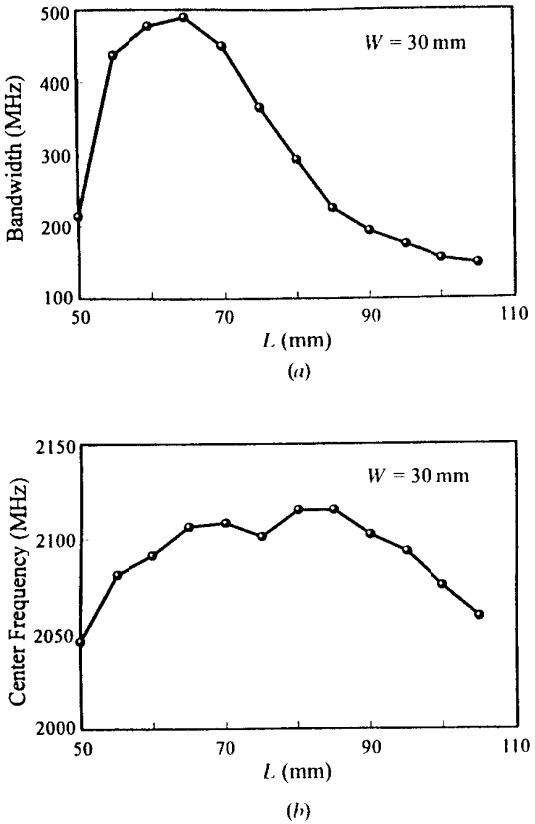

FIGURE 2.46 Measured (a) impedance bandwidth and (b) center operating frequency for the PIFA shown in Figure 2.44 with $W = 30$ mm. (From Ref. 21, © 2002 John Wiley & Sons, Inc.)

when the ground-plane width is smaller than 40 mm (about 27% of the free space wavelength at 2050 MHz), a relatively very sharp variation from about 1945 to 2105 MHz for the center operating frequency is observed for a small variation of 10 mm (W from 40 to 30 mm). Similarly, for W varied from 40 to 30 mm, the variations in the measured impedance bandwidth are as large as about 250 MHz (from about 240 to 490 MHz). This suggests that there exists a critical ground plane width for large variations in the impedance bandwidth and the center operating frequency of the PIFA. Also note that, because it becomes impractical for the ground plane width of a mobile phone to be smaller than 30 mm, the cases with W less than 30 mm are not studied.

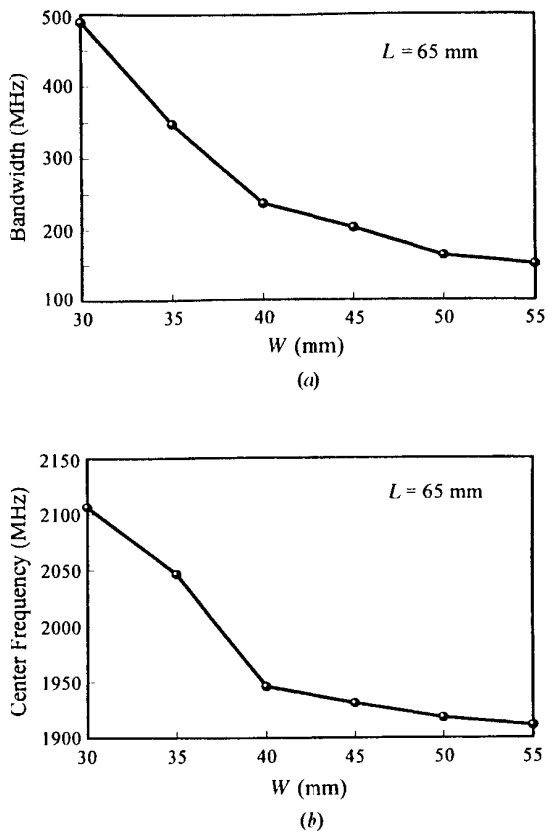

FIGURE 2.47 Measured (a) impedance bandwidth and (b) center operating frequency for the PIFA shown in Figure 2.44 with $L = 65$ mm. (From Ref. 21, © 2002 John Wiley & Sons, Inc.)

REFERENCES

1. Z. D. Liu, P. S. Hall, and D. Wake, "Dual-frequency planar inverted F antenna," IEEE Trans. Antennas Propagat., vol. 45, pp. 1451–1458, Oct. 1997.
2. C. R. Rowell and R. D. Murch, "A compact PIFA suitable for dual-frequency 900/1800-MHz operation," IEEE Trans. Antennas Propagat., vol. 46, pp. 596–598, April 1998.
3. S. Tarvas, J. Mikkola, S. Kivela, and A. Isohatala, "Planar dual-frequency antenna and radio apparatus employing a planar antenna," U.S. Patent No. 6252552, June 26, 2001.
4. S. Tarvas and A. Isohatala, "An internal dual-band mobile phone antenna," in 2000 IEEE Antennas Propagat. Soc. Int. Symp. Dig., pp. 266–269.

5. M. Martinez-Vazquez, M. Geissler, D. Heberling, A. Martinez-Gonzalez, and D. Sanchez-Hernandez, "Compact dual-band antenna for mobile handsets," Microwave Opt. Technol. Lett., vol. 32, pp. 87–88, Jan. 20, 2002.
6. P. Salonen, M. Keskilammi, and M. Kivikoski, "New slot configurations for dual-band planar inverted-F antenna," Microwave Opt. Technol. Lett., vol. 28, pp. 293–298, March 5, 2001.
7. N. Chiba, T. Amano, and H. Iwasaki, "Multifrequency inverted F-type antenna," U.S. Patent No. 6195048, Feb. 27, 2001.
8. F. R. Hsiao, H. T. Chen, G. Y. Lee, T. W. Chiou, and K. L. Wong, "A dual-band planar inverted-F patch antenna with a branch-line slit," Microwave Opt. Technol. Lett., vol. 32, pp. 310–312, Feb. 20, 2002.
9. W. Dou and W. Y. M. Chia, "Novel single-feed dual-band planar inverted-F antenna with a slot," in Proc. 2000 Int. Symp. Antennas Propagat. (ISAP), pp. 1115–1118
10. J. Ollikainen, O. Lehmus, M. Fischer, and P. Vainikainen, "Internal dual-band patch antenna for mobile phones," in Proc. Millennium Conf. on Antennas Propagat., Davos, Switzerland, p. 364.
11. D. Manteuffel, A. Bahr, D. Heberling, and I. Wolff, "Design considerations for integrated mobile phone antennas," in Proc. 2001 Int. Conf. on Antennas Propagat. (ICAP), pp. 252–254.
12. S. T. Fang, S. H. Yeh, and K. L. Wong, "Planar Inverted-F antennas for GSM/DCS mobile phones and dual ISM-band applications," in 2002 IEEE Antennas Propagat. Soc. Int. Symp. Dig., vol. 4, pp. 524–527.
13. G. H. K. Lui and R. D. Murch, "Compact dual-frequency PIFA designs using LC resonators," IEEE Trans. Antennas Propagat., vol. 49, pp. 1016–1019, July 2001.
14. S. H. Yeh and K. L. Wong, "Compact dual-frequency PIFA with a chip-inductor-loaded rectangular spiral strip," Microwave Opt. Technol. Lett., vol. 33, pp. 394–397, June 20, 2002.
15. C. T. P. Song, P. S. Hall, H. Ghafouri-Shiraz, and D. Wake, "Triple band planar inverted F antennas for handheld devices," Electron. Lett., vol. 36, pp. 112–114, Jan. 20, 2000.
16. W. P. Dou and Y. W. M. Chia, "Novel meandered planar inverted-F antenna for triple-frequency operation," Microwave Opt. Technol. Lett., vol. 27, pp. 58–60, Oct. 5, 2000.
17. F. R. Hsiao and K. L. Wong, "Compact planar inverted-F patch antenna for triple-frequency operation," Microwave Opt. Technol. Lett., vol. 33, pp. 459–462, June 20, 2002.
18. F. R. Hsiao and K. L. Wong, "A shorted patch antenna with an L-shaped ground plane for internal mobile handset antenna," Microwave Opt. Technol. Lett., vol. 33, pp. 314–316, May 20, 2002.
19. J. Ollikainen, M. Fischer, and P. Vainikainen, "Thin dual-resonant stacked shorted patch antenna for mobile communications," Electron. Lett., vol. 35, pp. 437–438, March 18, 1999.
20. G. Y. Lee, T. W. Chiou, and K. L. Wong, "Broadband stacked shorted patch antenna for mobile communication handsets," in Proc. 2001 Asia-Pacific Microwave Conf., pp. 232–235.
21. T. Y. Wu and K. L. Wong, "On the impedance bandwidth of a planar inverted-F antenna for mobile handsets," Microwave Opt. Technol. Lett., vol. 32, pp. 249–251, Feb. 20, 2002.

22. K. L. Wong and W. S. Chen, "Compact microstrip antenna with dual-frequency operation," Electron. Lett., vol. 33, pp. 646–647, April 10, 1997.
23. C. L. Tang, H. T. Chen, and K. L. Wong, "Small circular microstrip antenna with dual-frequency operation," Electron. Lett., vol. 33, pp. 1112–1113, June 19, 1997.